Model Based Control of Compact Heat Exchangers Independent of the Heat Transfer Behavior

authored by **A. Michel and A. Kugi**

and published in *Journal of Process Control*.

Cite this article as:

A. Michel and A. Kugi, "Model based control of compact heat exchangers independent of the heat transfer behavior", *Journal of Process Control*, vol. 50, no. 11-12, pp. 1859–1868, 2014. DOI: 10.1016/j.jprocont.2014.02.003

BibTex entry:

```
@ARTICLE{MichelJPC2014,
    author = {Michel, A. and Kugi, A.},
    title = {Model Based Control of Compact Heat Exchangers Independent of the Heat Transfer Behavior},
    journal = {Journal of Process Control},
    year = {2014},
    volume = {50},
    number = {11-12},
    pages = {1859-1868},
    doi = {10.1016/j.jprocont.2014.02.003},
    url = {http://www.sciencedirect.com/science/article/pii/S0959152414000456}
}
```

Link to original paper:

http://dx.doi.org/10.1016/j.jprocont.2014.02.003
http://www.sciencedirect.com/science/article/pii/S0959152414000456

Contact:

Automation and Control Institute (ACIN)	Internet:	www.acin.tuwien.ac.at
Vienna University of Technology	E-mail:	office@acin.tuwien.ac.at
Gusshausstrasse 27-29/E376	Phone:	+43 1 58801 37601
1040 Vienna, Austria	Fax:	+43 1 58801 37699

Model Based Control of Compact Heat Exchangers Independent of the Heat Transfer Behavior

Alexander Michel*, Andreas Kugi

Automation and Control Institute (ACIN), Vienna University of Technology, Gußhausstraße 27-29 / E376, 1040 Vienna, Austria

Abstract

Compact heat exchangers have a wide range of applications where standard control strategies typically rely on the knowledge of the heat transfer model and thus on the overall heat transfer coefficient. In particular for compact plate heat exchangers, the overall heat transfer coefficient strongly varies with the manufacturer's plate design and has to be identified by means of extensive measurements. This paper presents an alternative approach for the control of compact heat exchangers which can be implemented without the knowledge of the heat transfer behavior and is robust against changes in the coolant supply system. For this, a model based control strategy is presented which relies on the total thermal energy stored in the fluids of the heat exchanger as control variable instead of the outlet temperature. Furthermore, two methods are developed in order to estimate the total thermal energy, one based on a Kalman Filter and the other one on quasi-static considerations. Finally, the proposed control and estimation strategies are validated by means of simulation and measurement results on an industrial plate heat exchanger.

Keywords: Energy control, compact heat exchanger, finite volume method, independency of the overall heat transfer coefficient

1. Introduction

Industrial fluid-fluid temperature control systems have a wide range of applications, e.g. in food industry, for hydraulic oil cooling, in district heating, or for the cooling of machine tools. The typical design of such an industrial fluid-fluid cooling system is depicted in Figure 1. It consists of two fluid circuits which are thermally coupled by a heat exchanger. The first circuit, henceforth denoted by I, is connected to the process and the second circuit, marked with II, is connected to a coolant supply. The aim of the system is to keep the fluid temperature supplied to the process at a desired level. Usually, the flow rate of circuit II serves as a control input, which, for instance, can be adjusted by a proportional valve. In general, the temperature of the coolant supply cannot be controlled but can vary depending on the setup of the coolant supply and other thermal loads. Neglecting the heat exchange with the environment, the task of controlling the fluid-fluid cooling system reduces to a regulation of the outlet temperature of circuit I of the heat exchanger. In particular for the cooling of machine tools, compact systems with brazed plate heat exchangers are often employed. Apart from their compact design, they have the advantage of a very high overall heat transfer coefficient.

Controlling the outlet temperature of a heat exchanger has been extensively discussed in the literature. Apart from the different control strategies used, the contributions also differ in the choice of the control input. In [11]

*Corresponding author: Tel.: +43 1 58801 376 21, fax: +43 1 58801 376 99

Email addresses: michel@acin.tuwien.ac.at (Alexander Michel), kugi@acin.tuwien.ac.at (Andreas Kugi)

URL: http://www.acin.tuwien.ac.at (Alexander Michel)

Postprint submitted to Journal of Process Control

Post-print version of the article: A. Michel and A. Kugi, "Model based control of compact heat exchangers independent of the heat transfer behavior", *Journal of Process Control*, vol. 50, no. 11-12, pp. 1859–1868, 2014. DOI: 10.1016/j.jprocont.2014.02.003

Nomenclature

A_c cross section [m^2]
$\mathbf{A}, \mathbf{B}, \mathbf{C}, \mathbf{D}$ finite volume matrices
b channel width [m]
C_{Nu} correlation parameter
c_p specific heat capacity [J/(kg K)]
d_h hydraulic diameter [m]
d_p plate heigth [m]
E_Σ total thermal energy [J]
h heat transfer coefficient [W/(m^2 K)]
k thermal conductivity [W/(m K)]
l channel length [m]
M number of discretization elements
n_{Pr} correlation parameter
n_{Re} correlation parameter
Nu Nusselt number $Nu = hd_h/k$
Pr Prandtl number $Pr = \mu c_p/k$
$\dot{\mathrm{q}}$ heat flux density [W/m^2]
q flow rate [m^3/s]
Re Reynolds number $Re = |u|\varrho d_h/\mu$
t time [s]
T_s sampling time
u flow velocity [m/s]
U overall heat transfer coefficient [W/(m^2 K)]
V overall volume [m^3]
x coordinate in length direction [m]
z coordinate in thickness direction [m]

Greek Symbols
α abbreviation (see (2) and (9)) [m^2 K/J]
$\Delta\bar{\vartheta}$ mean temperature difference [K]
$\Delta\vartheta_{m,log}$ log. mean temperature difference [K]
μ dynamic viscosity [kg/(m s)]
ϑ temperature [K]
λ_1, λ_2 controller parameters
ϱ mass density [kg/m^3]
$\boldsymbol{\theta}$ state vector of the finite volume model
ξ abbreviation (see (A.5)-(A.7))

Subscripts
I side I of the heat exchanger
II side II of the heat exchanger
p plate

Superscripts
d desired
eff effective
in inlet
out outlet
- (overbar) mean value

an input-output linearization is developed for a countercurrent heat exchanger, using both the inlet temperature of circuit II and the fluid velocity of circuit I as control inputs. This approach was extended to cocurrent heat exchangers in [12]. A flatness based feedforward control concept based on a distributed-parameter model with the inlet temperature of circuit II as control input is presented in [18]. Moreover, many contributions can be found which use the fluid velocity of circuit II as control input. For instance [6] proposes a fuzzy model based approach with a predictive controller. Besides, [1] compares fuzzy controllers with conventional PI and PID controllers tuned on a first-principles model. Furthermore, in [19] a simple-to-implement control strategy is designed which does not require any system parameters and ensures stability but lacks in dynamics compared to more advanced strategies. In addition, a number of papers is concerned with control strategies relying on physics based mathematical models with different degree of accuracy. While in [2] a repetitive controller is designed in the frequency domain, in [10] an optimal control strategy is developed based on a discrete time-delay approximation of the transport phenomenon of the heat exchanger. Moreover, many model based control concepts are applied to lumped-parameter models with only 2 states, as it is the case in [13] which proposes an exact input-output linearization.

Despite the many control strategies proposed in literature, the inherent nonlinear dependence of the overall heat transfer coefficient on the flow rates is neglected in the majority of cases. However, the application of model based control strategies typically requires the exact knowledge of the overall heat transfer coefficient in particular for brazed plate heat exchangers. The plates of this type of heat exchanger are specifically designed to yield a high turbulent velocity field, which in turn entails high values of the overall heat transfer coefficient strongly depending on the flow rates. A functional description of the overall heat transfer coefficient based on analytical considerations can hardly be found. Thus, typically semi-empirical relations are used which require extensive identification. Moreover, even if this relation was exactly known for the nominal heat exchanger, it may strongly change over lifetime due to fouling effects. This necessitates a repeated calibration of the model during operation.

In this paper, an alternative control strategy is developed. Though the controller relies on a physics based mathematical model, it can be implemented without the knowledge of the overall heat transfer coefficient. This can

Post-print version of the article: A. Michel and A. Kugi, "Model based control of compact heat exchangers independent of the heat transfer behavior", *Journal of Process Control*, vol. 50, no. 11-12, pp. 1859–1868, 2014. DOI: 10.1016/j.jprocont.2014.02.003
The content of this post-print version is identical to the published paper but without the publisher's final layout or copy editing.

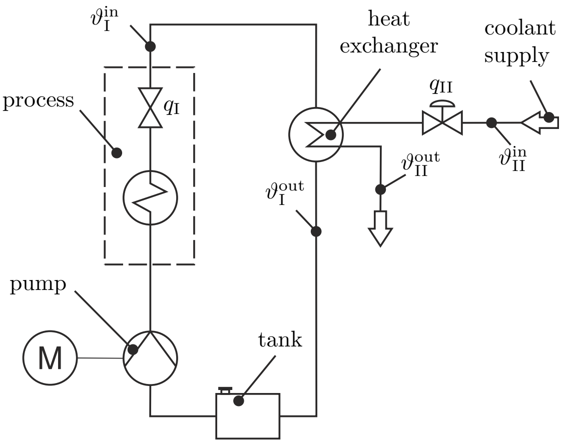

Figure 1: Schematic design of the cooling system.

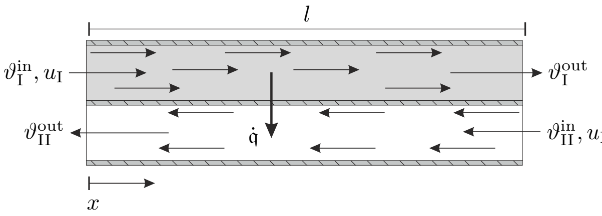

Figure 2: Simplified heat exchanger geometry for a countercurrent flow arrangement.

be achieved by controlling the total thermal energy stored in the heat exchanger. Because the latter cannot be measured, two approaches, one based on a Kalman Filter and the other on a quasi-static approximation, are proposed.

The paper is structured as follows: In Section 2, the mathematical model of the heat exchanger is developed based on the fundamentals of convective heat transfer. In Section 3, a controller is derived from the spatially averaged distributed-parameter model of the heat exchanger using the thermal energy stored inside the heat exchanger as control variable. In order to determine the stored thermal energy, two methods are presented: (i) a Kalman Filter based on an early-lumping approximation of the distributed-parameter model of the heat exchanger, and (ii) an approach which utilizes quasi-static considerations. Finally, the control strategy and both estimation concepts are validated by means of simulation and measurement results in Section 4. The paper ends with some conclusions.

2. Modeling

In the following, the convection and the heat transfer model of a compact fluid-fluid heat exchanger for a countercurrent and a cocurrent flow arrangement is summarized. For this, a simplified heat exchanger geometry is considered, which is depicted exemplary for a countercurrent flow arrangement in Figure 2.

2.1. Convection Model

If typical approximations in heat exchanger modeling are taken into account, such as (i) plug flow, (ii) constant temperature $\vartheta_{\mathrm{I}}(x,t)$ and $\vartheta_{\mathrm{II}}(x,t)$ over the cross section, (iii) no phase changes, (iv) constant material parameters, (v) no heat transfer with the environment, and (vi) neglect of heat conduction compared to convection along the flow direction, the mathematical model of both sides of the heat exchanger can be derived from the first law of thermodynamics [3] in the form

$$\frac{\partial \vartheta_{\mathrm{I}}}{\partial t} + u_{\mathrm{I}} \frac{\partial \vartheta_{\mathrm{I}}}{\partial x} = \alpha_{\mathrm{I}} \dot{\mathfrak{q}}_{\mathrm{I}} \tag{1a}$$

$$\frac{\partial \vartheta_{\mathrm{II}}}{\partial t} + u_{\mathrm{II}} \frac{\partial \vartheta_{\mathrm{II}}}{\partial x} = \alpha_{\mathrm{II}} \dot{\mathfrak{q}}_{\mathrm{II}} \tag{1b}$$

with

$$\alpha_{\mathrm{I}} = \frac{b}{A_{c,\mathrm{I}} \varrho_{\mathrm{I}} c_{p,\mathrm{I}}}, \qquad \alpha_{\mathrm{II}} = \frac{b}{A_{c,\mathrm{II}} \varrho_{\mathrm{II}} c_{p,\mathrm{II}}}\ , \tag{2}$$

the boundary conditions

$$\vartheta_{\mathrm{I}}^{\mathrm{in}} = \begin{cases} \vartheta_{\mathrm{I}}(0,t) & \text{for } u_{\mathrm{I}} > 0 \\ \vartheta_{\mathrm{I}}(l,t) & \text{for } u_{\mathrm{I}} < 0 \end{cases} \tag{3a}$$

$$\vartheta_{\mathrm{II}}^{\mathrm{in}} = \begin{cases} \vartheta_{\mathrm{II}}(0,t) & \text{for } u_{\mathrm{II}} > 0 \\ \vartheta_{\mathrm{II}}(l,t) & \text{for } u_{\mathrm{II}} < 0\ , \end{cases} \tag{3b}$$

and appropriate initial conditions. Here $\vartheta_{\mathrm{I}}^{\mathrm{in}}$ and $\vartheta_{\mathrm{II}}^{\mathrm{in}}$ denote the fluid temperatures at the inlet of the heat exchanger, $\dot{\mathfrak{q}}_{\mathrm{I}}$ and $\dot{\mathfrak{q}}_{\mathrm{II}}$ the heat flux densities supplied to each channel and u_{I} and u_{II} are the fluid velocities. Furthermore, b denotes the width of the channel, $A_{c,\mathrm{I}}$ and $A_{c,\mathrm{II}}$ the cross sections, ϱ_{I} and ϱ_{II} the fluid densities and $c_{p,\mathrm{I}}$, $c_{p,\mathrm{II}}$ the specific heat capacities of side I and side II, respectively. The two sides of the heat exchanger are thermally coupled via $\dot{\mathfrak{q}}_{\mathrm{I}}$ and $\dot{\mathfrak{q}}_{\mathrm{II}}$. Note that the heat exchanger model (1) with the boundary conditions (3) covers the countercurrent and the cocurrent flow arrangement, which only differ in the sign of the fluid velocities. If $\operatorname{sign}(u_{\mathrm{I}}) = -\operatorname{sign}(u_{\mathrm{II}})$ the heat exchanger is in a countercurrent flow arrangement and if $\operatorname{sign}(u_{\mathrm{I}}) = \operatorname{sign}(u_{\mathrm{II}})$ it is in a cocurrent flow arrangement. All following calculations are independent of the actual flow configuration, unless it is stated otherwise in the text.

2.2. Thermal Coupling

In order to model the thermal coupling between the two channels, the temperature field near the dividing plate of height d_p is essential, see Figure 3 for $\vartheta_{\mathrm{I}} > \vartheta_{\mathrm{II}}$. This temperature field strongly depends on the velocity field near the plate, see [7], which acts as a variable thermal resistance. As it is depicted in Figure 3, the heat fluxes $\dot{\mathfrak{q}}_{\mathrm{I}}$ and

Post-print version of the article: A. Michel and A. Kugi, “Model based control of compact heat exchangers independent of the heat transfer behavior”, *Journal of Process Control*, vol. 50, no. 11-12, pp. 1859–1868, 2014. DOI: 10.1016/j.jprocont.2014.02.003

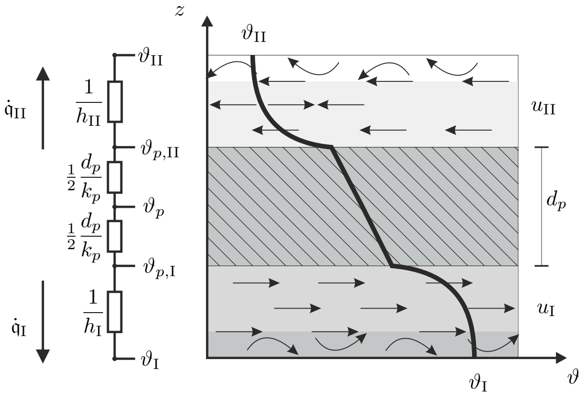

Figure 3: Heat transfer model.

$\dot{q}_{II}$ between the fluids and the dividing plate have to pass this thermal resistance and can be calculated according to Newton's law of cooling

$$\dot{q}_I = -h_I (\vartheta_I - \vartheta_{p,I}) \ , \tag{4a}$$
$$\dot{q}_{II} = -h_{II} (\vartheta_{II} - \vartheta_{p,II}) \ . \tag{4b}$$

Thereby, $\vartheta_{p,I}$ and $\vartheta_{p,II}$ denote the temperature of the plate in contact with fluid I and II, respectively. Furthermore, h_I and h_{II} are known as heat transfer coefficients. The precise values of the heat transfer coefficients can be determined analytically only for very simplistic scenarios, which is why in practical applications usually the semi-empirical similitude theory according to Nusselt is employed. This method relies on a suitable approximation of the functional relation of the Nusselt number Nu, on the Prandtl number Pr and the Reynolds number Re [7], i.e.,

$$Nu = Nu(Pr, Re) \tag{5}$$

with

$$Nu = \frac{hd_h}{k} \ , \qquad Pr = \frac{\mu c_p}{k} \ , \qquad Re = \frac{|u|\varrho d_h}{\mu} \ , \tag{6}$$

and the hydraulic diameter d_h, the fluid thermal conductivity k and the dynamic viscosity μ. Many relations for the so called Nusselt correlation (5) depending on the specific design of the respective heat exchanger type are given in literature, see, e.g., [9, 15, 17]. However, they all agree in the fact that

$$Nu(Pr, Re > 0) > 0 \tag{7}$$

and that the arising parameters have to be identified by means of suitable measurements.

Usually the dividing plates of a heat exchanger are quite thin with high thermal conductivity k_p. Thus it is possible to consider the temperature profile in z-direction in a quasi-static manner. A detailed analysis of typical compact heat exchangers shows that the heat conduction inside the plate in x-direction has only minor influence compared to the supplied heat from the fluids and can also be neglected. Then it is possible, see [14], by introducing the temperature $\vartheta_p(x,t)$ in the middle of the plate, to derive the temperature model of the plate in the form

$$\frac{\partial \vartheta_p}{\partial t} = \alpha_p h_{I,p} (\vartheta_I - \vartheta_p) + \alpha_p h_{II,p} (\vartheta_{II} - \vartheta_p) \tag{8}$$

with

$$\alpha_p = \frac{1}{d_p \varrho_p c_{p,p}} \tag{9}$$

and

$$\frac{1}{h_{I,p}} = \frac{1}{h_I} + \frac{1}{2}\frac{d_p}{k_p}, \qquad \frac{1}{h_{II,p}} = \frac{1}{h_{II}} + \frac{1}{2}\frac{d_p}{k_p} \ , \tag{10}$$

whereby ϱ_p denotes the density and $c_{p,p}$ the specific heat capacity of the plate. In most cases, the heat capacity per length of the dividing plate and thus $\frac{1}{\alpha_p}$ is quite small, which is why the corresponding dynamics can be neglected. Then the heat flux density exchanged by the two fluids $\dot{q}$ reads as

$$\dot{q} = \dot{q}_{II} = -\dot{q}_I = U (\vartheta_I - \vartheta_{II}) \tag{11}$$

with the so called overall heat transfer coefficient

$$\frac{1}{U} = \frac{1}{h_{I,p}} + \frac{1}{h_{II,p}} = \frac{1}{h_I} + \frac{d_p}{k_p} + \frac{1}{h_{II}} \ . \tag{12}$$

2.3. Heat Exchanger Model

Combining the findings of the previous section, the mathematical model of a compact fluid-fluid heat exchanger can be written as a distributed-parameter system, see [14] for more details,

$$\frac{\partial \vartheta_I}{\partial t} + u_I \frac{\partial \vartheta_I}{\partial x} = -\alpha_I h_{I,p} (\vartheta_I - \vartheta_p) \tag{13a}$$
$$\frac{\partial \vartheta_p}{\partial t} = \alpha_p h_{I,p} (\vartheta_I - \vartheta_p) + \alpha_p h_{II,p} (\vartheta_{II} - \vartheta_p) \tag{13b}$$
$$\frac{\partial \vartheta_{II}}{\partial t} + u_{II} \frac{\partial \vartheta_{II}}{\partial x} = -\alpha_{II} h_{II,p} (\vartheta_{II} - \vartheta_p) \tag{13c}$$

with the boundary conditions (3) and appropriate initial conditions. If the heat capacity of the plate is negligible, (13) simplifies to

$$\frac{\partial \vartheta_I}{\partial t} = -u_I \frac{\partial \vartheta_I}{\partial x} - \alpha_I U (\vartheta_I - \vartheta_{II}) \tag{14a}$$
$$\frac{\partial \vartheta_{II}}{\partial t} = -u_{II} \frac{\partial \vartheta_{II}}{\partial x} - \alpha_{II} U (\vartheta_{II} - \vartheta_I) \ . \tag{14b}$$

Note that according to (5), (6) and (10), the heat transfer coefficients $h_{I,p}$ and $h_{II,p}$ and thus the overall heat transfer coefficient U due to (12) directly depend on the fluid velocities u_I and u_{II} in a nonlinear manner. Furthermore, the Nusselt correlation (5) is a semi-empirical relation, which is different for any type of heat exchanger and in most cases not simple to parameterize. The required identifications are in general quite extensive, in particular if the variety of products to be considered is high.

Post-print version of the article: A. Michel and A. Kugi, "Model based control of compact heat exchangers independent of the heat transfer behavior", *Journal of Process Control*, vol. 50, no. 11-12, pp. 1859–1868, 2014. DOI: 10.1016/j.jprocont.2014.02.003

3. Control Strategy

The main idea of the control strategy developed in this paper relies on the fact that, instead of directly controlling the outlet temperature $\vartheta_{\mathrm{I}}^{\mathrm{out}}$, the total thermal energy stored in the fluids of the heat exchanger serves as the control variable. This results in a control law that is independent of the overall heat transfer coefficient U.

3.1. Controller Design Model

In a first step, the mathematical model (14) with the boundary conditions (3) is integrated over the length l of the heat exchanger resulting in the following system of ordinary differential equations[1]

$$\dot{\bar{\vartheta}}_{\mathrm{I}} = -\frac{q_{\mathrm{I}}}{V_{\mathrm{I}}}\left(\vartheta_{\mathrm{I}}^{\mathrm{out}} - \vartheta_{\mathrm{I}}^{\mathrm{in}}\right) - \alpha_{\mathrm{I}} U \left(\bar{\vartheta}_{\mathrm{I}} - \bar{\vartheta}_{\mathrm{II}}\right) \tag{15a}$$

$$\dot{\bar{\vartheta}}_{\mathrm{II}} = -\frac{q_{\mathrm{II}}}{V_{\mathrm{II}}}\left(\vartheta_{\mathrm{II}}^{\mathrm{out}} - \vartheta_{\mathrm{II}}^{\mathrm{in}}\right) - \alpha_{\mathrm{II}} U \left(\bar{\vartheta}_{\mathrm{II}} - \bar{\vartheta}_{\mathrm{I}}\right) \tag{15b}$$

with the mean temperature values

$$\bar{\vartheta}_{\mathrm{I}} = \frac{1}{l}\int_0^l \vartheta_{\mathrm{I}} \mathrm{d}x, \quad \bar{\vartheta}_{\mathrm{II}} = \frac{1}{l}\int_0^l \vartheta_{\mathrm{II}} \mathrm{d}x \ . \tag{16}$$

Furthermore, the flow rates q_{I} and q_{II} read as

$$q_{\mathrm{I}} = |u_{\mathrm{I}}| A_{c,\mathrm{I}}, \quad q_{\mathrm{II}} = |u_{\mathrm{II}}| A_{c,\mathrm{II}} \ , \tag{17}$$

the inlet temperatures $\vartheta_{\mathrm{I}}^{\mathrm{in}}$ and $\vartheta_{\mathrm{II}}^{\mathrm{in}}$ are due to (3), the outlet temperatures $\vartheta_{\mathrm{I}}^{\mathrm{out}}$ and $\vartheta_{\mathrm{II}}^{\mathrm{out}}$ are given by

$$\vartheta_{\mathrm{I}}^{\mathrm{out}} = \begin{cases} \vartheta_{\mathrm{I}}(l,t) & \text{for } u_{\mathrm{I}} > 0 \\ \vartheta_{\mathrm{I}}(0,t) & \text{for } u_{\mathrm{I}} < 0 \end{cases} \tag{18a}$$

$$\vartheta_{\mathrm{II}}^{\mathrm{out}} = \begin{cases} \vartheta_{\mathrm{II}}(l,t) & \text{for } u_{\mathrm{II}} > 0 \\ \vartheta_{\mathrm{II}}(0,t) & \text{for } u_{\mathrm{II}} < 0 \end{cases} \tag{18b}$$

and the overall volumes V_{I} and V_{II} of side I and side II, respectively, take the form

$$V_{\mathrm{I}} = l A_{c,\mathrm{I}} \ , \qquad V_{\mathrm{II}} = l A_{c,\mathrm{II}} \ . \tag{19}$$

Introducing the total thermal energy stored in the two fluids inside the heat exchanger

$$E_{\Sigma} = c_{p,\mathrm{I}} \varrho_{\mathrm{I}} V_{\mathrm{I}} \bar{\vartheta}_{\mathrm{I}} + c_{p,\mathrm{II}} \varrho_{\mathrm{II}} V_{\mathrm{II}} \bar{\vartheta}_{\mathrm{II}} \tag{20}$$

and the mean temperature difference

$$\Delta\bar{\vartheta} = \bar{\vartheta}_{\mathrm{I}} - \bar{\vartheta}_{\mathrm{II}} \ , \tag{21}$$

(15) can be written in the form

$$\dot{E}_{\Sigma} = c_{p,\mathrm{II}} \varrho_{\mathrm{II}} q_{\mathrm{II}} \left(\vartheta_{\mathrm{II}}^{\mathrm{in}} - \vartheta_{\mathrm{II}}^{\mathrm{out}}\right) - c_{p,\mathrm{I}} \varrho_{\mathrm{I}} q_{\mathrm{I}} \left(\vartheta_{\mathrm{I}}^{\mathrm{out}} - \vartheta_{\mathrm{I}}^{\mathrm{in}}\right) \tag{22a}$$

$$\begin{aligned} \Delta\dot{\bar{\vartheta}} = {} & \frac{q_{\mathrm{II}}}{V_{\mathrm{II}}}\left(\vartheta_{\mathrm{II}}^{\mathrm{out}} - \vartheta_{\mathrm{II}}^{\mathrm{in}}\right) - \frac{q_{\mathrm{I}}}{V_{\mathrm{I}}}\left(\vartheta_{\mathrm{I}}^{\mathrm{out}} - \vartheta_{\mathrm{I}}^{\mathrm{in}}\right) \\ & - U\left(\alpha_{\mathrm{I}} + \alpha_{\mathrm{II}}\right)\Delta\bar{\vartheta} \ . \end{aligned} \tag{22b}$$

[1]Remember that U depends on q_{I} and q_{II} in a highly nonlinear manner, cf. (5), (6) and (12).

Henceforth, (22) will serve as the controller design model. Clearly, the outlet temperatures $\vartheta_{\mathrm{I}}^{\mathrm{out}}$ and $\vartheta_{\mathrm{II}}^{\mathrm{out}}$ depend on the mean temperature values $\bar{\vartheta}_{\mathrm{I}}$ and $\bar{\vartheta}_{\mathrm{II}}$ and thus on E_{Σ} and $\Delta\bar{\vartheta}$, respectively. Note that, except for the quasi-static case, it is not possible to find an explicit relation between $\vartheta_{\mathrm{I}}^{\mathrm{out}}$, $\vartheta_{\mathrm{II}}^{\mathrm{out}}$ and E_{Σ}, $\Delta\bar{\vartheta}$. However, if the outlet temperatures can be measured, their influence can be compensated in the control law.

3.2. Energy Control

Let us first assume that the total energy E_{Σ} according to (20) and its desired value E_{Σ}^d are known. Then the control law

$$\frac{\mathrm{d}}{\mathrm{d}t} e_1 = E_{\Sigma} - E_{\Sigma}^d \tag{23a}$$

$$q_{\mathrm{II}} = -\frac{c_{p,\mathrm{I}} \varrho_{\mathrm{I}} q_{\mathrm{I}} \left(\vartheta_{\mathrm{I}}^{\mathrm{out}} - \vartheta_{\mathrm{I}}^{\mathrm{in}}\right) - \lambda_2 e_2 - \lambda_1 e_1}{c_{p,\mathrm{II}} \varrho_{\mathrm{II}} \left(\vartheta_{\mathrm{II}}^{\mathrm{out}} - \vartheta_{\mathrm{II}}^{\mathrm{in}}\right)} \ , \tag{23b}$$

applied to (22a) leads to the globally exponentially stable error system

$$\frac{\mathrm{d}}{\mathrm{d}t} \underbrace{\begin{bmatrix} e_1 \\ e_2 \end{bmatrix}}_{\mathbf{e}_{\Sigma}} = \underbrace{\begin{bmatrix} 0 & 1 \\ -\lambda_1 & -\lambda_2 \end{bmatrix}}_{\mathbf{A}_{\Sigma}} \begin{bmatrix} e_1 \\ e_2 \end{bmatrix} \tag{24}$$

with $e_2 = E_{\Sigma} - E_{\Sigma}^d$, $\lambda_1, \lambda_2 > 0$ and the Hurwitz matrix $\mathbf{A}_{\Sigma}$. The closed-loop system (22) and (23) reads as

$$\dot{\mathbf{e}}_{\Sigma} = \mathbf{A}_{\Sigma} \mathbf{e}_{\Sigma} \tag{25a}$$

$$\Delta\dot{\bar{\vartheta}} = -a(t)\Delta\bar{\vartheta} + \frac{1}{c_{p,\mathrm{II}} \varrho_{\mathrm{II}} V_{\mathrm{II}}} \boldsymbol{\lambda}^{\mathrm{T}} \mathbf{e}_{\Sigma} + d(t) \ , \tag{25b}$$

with

$$a(t) = U\left(\alpha_{\mathrm{I}} + \alpha_{\mathrm{II}}\right) \ , \tag{26a}$$

$$d(t) = -\left(\frac{c_{p,\mathrm{I}} \varrho_{\mathrm{I}}}{c_{p,\mathrm{II}} \varrho_{\mathrm{II}} V_{\mathrm{II}}} + \frac{1}{V_{\mathrm{I}}}\right) q_{\mathrm{I}} \left(\vartheta_{\mathrm{I}}^{\mathrm{out}} - \vartheta_{\mathrm{I}}^{\mathrm{in}}\right) \tag{26b}$$

and $\boldsymbol{\lambda}^{\mathrm{T}} = [\lambda_1, \lambda_2]$. Since from an operational point of view the inlet temperatures $\vartheta_{\mathrm{I}}^{\mathrm{in}}$, $\vartheta_{\mathrm{II}}^{\mathrm{in}}$, the outlet temperatures $\vartheta_{\mathrm{I}}^{\mathrm{out}}$, $\vartheta_{\mathrm{II}}^{\mathrm{out}}$ and the flow rates q_{I}, q_{II} are positive and bounded, i.e. $a(t) \geq a_{min} > 0$ and $|d(t)| < d_{max}$ for all times t, it can be deduced that $\Delta\bar{\vartheta}$ remains bounded. In fact the solution of (25b) can be written in the form

$$\begin{aligned} \Delta\bar{\vartheta}(t) = {} & \Delta\bar{\vartheta}(t_0)\exp\left(-\int_{t_0}^t a(\tau)\mathrm{d}\tau\right) \\ & + \int_{t_0}^t d(\tau)\exp\left(-\int_{\tau}^t a(r)\mathrm{d}r\right)\mathrm{d}\tau \\ & + \int_{t_0}^t \frac{1}{c_{p,\mathrm{II}} \varrho_{\mathrm{II}} V_{\mathrm{II}}} \boldsymbol{\lambda}^{\mathrm{T}} \mathbf{e}_{\Sigma}(\tau)\exp\left(-\int_{\tau}^t a(r)\mathrm{d}r\right)\mathrm{d}\tau \end{aligned} \tag{27}$$

and thus

$$\begin{aligned} |\Delta\bar{\vartheta}(t)| \leq {} & \left(\Delta\bar{\vartheta}(t_0) - \frac{\tilde{d}_{max}}{a_{min}}\right)\exp\left(-a_{min}(t - t_0)\right) \\ & + \frac{\tilde{d}_{max}}{a_{min}} \end{aligned} \tag{28}$$

Post-print version of the article: A. Michel and A. Kugi, "Model based control of compact heat exchangers independent of the heat transfer behavior", *Journal of Process Control*, vol. 50, no. 11-12, pp. 1859–1868, 2014. DOI: 10.1016/j.jprocont.2014.02.003
The content of this post-print version is identical to the published paper but without the publisher's final layout or copy editing.

with

$$\tilde{d}_{max} = d_{max} + \frac{1}{c_{p,\mathrm{II}}\varrho_{\mathrm{II}}V_{\mathrm{II}}}\sup_{\tau\geq t_0}\boldsymbol{\lambda}^{\mathrm{T}}\mathbf{e}_{\Sigma}(\tau)\ . \tag{29}$$

Note that $\mathbf{e}_{\Sigma}(\tau) = \exp\left(\mathbf{A}_{\Sigma}\left(\tau - t_0\right)\right)\mathbf{e}_{\Sigma}(t_0)$ is the solution of (24) for the initial condition $\mathbf{e}_{\Sigma}(t_0)$ which exponentially converges to zero since $\mathbf{A}_{\Sigma}$ is Hurwitz.

Though the implementation of the control law (23) is quite simple, the actual value of the total thermal energy E_{Σ} stored in the system has to be known. Therefore, an observer is designed in order to estimate the not directly measurable value of E_{Σ}. Although some late-lumping approaches for the observer design of two coupled hyperbolic partial differential equations do exist in the recent literature, see, e.g., [16], the majority relies on an early-lumping approach, see, e.g., [4, 8, 11]. Thereby, the underlying partial differential equation is semi-discretized and for the resulting system of (nonlinear) ordinary differential equations classical observer strategies can be employed.

Henceforth, such an approach will be pursued in the first step. However, it turns out that the observer also depends on the exact knowledge of the heat transfer coefficient U and thus abolishes the asset of the proposed controller. Therefore, a further approach based on quasi-static considerations and the measurement of all inlet and outlet temperatures will be used in a second step.

3.3. Observer for the Determination of E_{Σ}

In the following, the finite volume method, which is commonly used for the semi-discretization of convective heat transfer problems, see, e.g., [5], will be applied to the reduced heat exchanger model (14). For this, the spatial domain of both sides of the heat exchanger is discretized in M elements. According to the finite volume method, the temperatures inside each discretization element are assumed to be constant and the temperatures at the borders of adjacent elements have to be interpolated. In doing so the utilized interpolation scheme has a strong influence on the dynamic and stationary accuracy of the resulting lumped-parameter system. Common methods, like the QUICK-interpolation [5], exhibit a good approximation regarding the transport phenomenon of the heat exchanger, but feature small stationary temperature errors which sum up and lead to wrong values of E_{Σ}. An alternative approach is given by the power balance scheme [14] which shows a high stationary accuracy.

Applying the finite volume method with the power balance scheme to the reduced heat exchanger model (14) yields

$$\begin{aligned}\frac{\mathrm{d}}{\mathrm{d}t}\boldsymbol{\theta} &= \mathbf{A}(\mathbf{u})\boldsymbol{\theta} + \mathbf{B}(\mathbf{u})\boldsymbol{\vartheta}^{\mathrm{in}}\\ \boldsymbol{\vartheta}^{\mathrm{out}} &= \mathbf{C}(\mathbf{u})\boldsymbol{\theta} + \mathbf{D}(\mathbf{u})\boldsymbol{\vartheta}^{\mathrm{in}}\end{aligned} \tag{30}$$

with

$$\mathbf{A}(\mathbf{u}) = \mathbf{A}_c(\mathbf{u}) + U(\mathbf{u})\mathbf{A}_t\ , \tag{31}$$

the state vector $\boldsymbol{\theta} = [\boldsymbol{\theta}_{\mathrm{I}}, \boldsymbol{\theta}_{\mathrm{II}}]^{\mathrm{T}}$, the input vectors $\mathbf{u} = [u_{\mathrm{I}}, u_{\mathrm{II}}]^{\mathrm{T}}$ and $\boldsymbol{\vartheta}^{\mathrm{in}} = \left[\vartheta_{\mathrm{I}}^{\mathrm{in}}, \vartheta_{\mathrm{II}}^{\mathrm{in}}\right]^{\mathrm{T}}$, and the output vector $\boldsymbol{\vartheta}^{\mathrm{out}} = [\vartheta_{\mathrm{I}}^{\mathrm{out}}, \vartheta_{\mathrm{II}}^{\mathrm{out}}]^{\mathrm{T}}$. The derivation of (30) as well as the matrices $\mathbf{A}_c$, $\mathbf{A}_t$, $\mathbf{B}$, $\mathbf{C}$ and $\mathbf{D}$ and the new state vector $\boldsymbol{\theta}$ are summarized in Appendix A. According to (20) the total thermal energy E_{Σ} of (30) can be directly determined from the state vector $\boldsymbol{\theta}$ in the form

$$\begin{aligned}E_{\Sigma} &= c_{p,\mathrm{I}}\varrho_{\mathrm{I}}V_{\mathrm{I}}\frac{1}{M}\sum_{i=1}^{M}\theta_{\mathrm{I}}^{i} + c_{p,\mathrm{II}}\varrho_{\mathrm{II}}V_{\mathrm{II}}\frac{1}{M}\sum_{i=1}^{M}\theta_{\mathrm{II}}^{i}\\ &= \mathbf{c}_{\Sigma}^{\mathrm{T}}\boldsymbol{\theta}\ ,\end{aligned} \tag{32}$$

with

$$\mathbf{c}_{\Sigma}^{\mathrm{T}} = \left[c_{p,\mathrm{I}}\varrho_{\mathrm{I}}V_{\mathrm{I}}\tfrac{1}{M}\mathbf{1}^{M\,\mathrm{T}} \quad c_{p,\mathrm{II}}\varrho_{\mathrm{II}}V_{\mathrm{II}}\tfrac{1}{M}\mathbf{1}^{M\,\mathrm{T}}\right]\ , \tag{33}$$

where θ_{I}^{i} and θ_{II}^{i} denote the entries of $\boldsymbol{\theta}_{\mathrm{I}}$ and $\boldsymbol{\theta}_{\mathrm{II}}$, respectively, and $\mathbf{1}^n = [1, 1, \ldots, 1, 1]^{\mathrm{T}} \in \mathbb{R}^n$. Using the forward Euler method for the time discretization of (30) with the sampling time T_s and extending the model with additive zero-mean Gaussian process noise $\mathbf{p}_k$ and measurement noise $\mathbf{n}_k$ leads to

$$\begin{aligned}\boldsymbol{\theta}_{k+1} &= \boldsymbol{\Phi}_k\boldsymbol{\theta}_k + \boldsymbol{\Gamma}_k\boldsymbol{\vartheta}_k^{\mathrm{in}} + \mathbf{p}_k\\ \boldsymbol{\vartheta}_k^{\mathrm{out}} &= \mathbf{C}_k\boldsymbol{\theta}_k + \mathbf{D}_k\boldsymbol{\vartheta}_k^{\mathrm{in}} + \mathbf{n}_k\end{aligned} \tag{34}$$

with

$$\boldsymbol{\Phi}_k = \mathbf{I}^{2M} + T_s\left(\mathbf{A}_c(\mathbf{u}_k) + U(\mathbf{u}_k)\mathbf{A}_t\right)\ , \tag{35a}$$
$$\boldsymbol{\Gamma}_k = T_s\mathbf{B}(\mathbf{u}_k), \tag{35b}$$
$$\mathbf{C}_k = \mathbf{C}(\mathbf{u}_k), \tag{35c}$$
$$\mathbf{D}_k = \mathbf{D}(\mathbf{u}_k) \tag{35d}$$

and $\boldsymbol{\theta}_k = \boldsymbol{\theta}(kT_s)$, $\mathbf{u}_k = \mathbf{u}(kT_s)$, $\boldsymbol{\vartheta}_k^{\mathrm{in}} = \boldsymbol{\vartheta}^{\mathrm{in}}(kT_s)$ and $\boldsymbol{\vartheta}_k^{\mathrm{out}} = \boldsymbol{\vartheta}^{\mathrm{out}}(kT_s)$. Furthermore, $\mathbf{I}^n \in \mathbb{R}^{n\times n}$ denotes the identity matrix. Using (34) as observer design model, a Kalman Filter can be derived in the form

$$\hat{\boldsymbol{\theta}}_{k+1} = \boldsymbol{\Phi}_k\hat{\boldsymbol{\theta}}_k + \boldsymbol{\Gamma}_k\boldsymbol{\vartheta}_k^{\mathrm{in}} + \hat{\mathbf{K}}_k\left(\boldsymbol{\vartheta}_k^{\mathrm{out}} - \mathbf{C}_k\hat{\boldsymbol{\theta}}_k - \mathbf{D}_k\boldsymbol{\vartheta}_k^{\mathrm{in}}\right) \tag{36a}$$
$$\hat{E}_{\Sigma,k} = \mathbf{c}_{\Sigma}^{\mathrm{T}}\hat{\boldsymbol{\theta}}_k\ , \tag{36b}$$

with the Kalman gain matrix

$$\hat{\mathbf{K}}_k = \boldsymbol{\Phi}_k\mathbf{P}_k\mathbf{C}_k^{\mathrm{T}}\left(\mathbf{C}_k\mathbf{P}_k\mathbf{C}_k^{\mathrm{T}} + \mathbf{R}\right)^{-1} \tag{37}$$

and the state error covariance matrix $\mathbf{P}_k$ as the solution of the Riccati equation

$$\mathbf{P}_{k+1} = \boldsymbol{\Phi}_k\mathbf{P}_k\boldsymbol{\Phi}^{\mathrm{T}} + \mathbf{Q} - \hat{\mathbf{K}}_k\mathbf{C}_k\mathbf{P}_k\boldsymbol{\Phi}_k^{\mathrm{T}} \tag{38}$$

with the positive definite covariance matrices $\mathbf{Q}$ and $\mathbf{R}$ of the process noise $\mathbf{p}_k$ and the measurement noise $\mathbf{n}_k$, respectively. In our case the matrices were chosen as $\mathbf{Q} = \mathrm{diag}([1, 1, \ldots, 1, 1]) \in \mathbb{R}^{2M\times 2M}$ and $\mathbf{R} = \mathrm{diag}([0.1, 0.1])$.

Post-print version of the article: A. Michel and A. Kugi, "Model based control of compact heat exchangers independent of the heat transfer behavior", *Journal of Process Control*, vol. 50, no. 11-12, pp. 1859–1868, 2014. DOI: 10.1016/j.jprocont.2014.02.003

3.4. Quasi-Static Approach for the Determination of E_Σ

In the case of compact heat exchangers, as shown in [14], it is possible to reduce the number of discretization elements M of the finite volume model (30) to only one single element without deteriorating the dynamic and stationary approximation accuracy. For $M = 1$, (30) with (17) simplifies to

$$\begin{bmatrix}\dot{\theta}_{\mathrm{I}}\\ \dot{\theta}_{\mathrm{II}}\end{bmatrix} = \left(\begin{bmatrix}-\frac{q_{\mathrm{I}}}{V_{\mathrm{I}}\xi_{\mathrm{I}}} & 0\\ 0 & -\frac{q_{\mathrm{II}}}{V_{\mathrm{II}}\xi_{\mathrm{II}}}\end{bmatrix} + U\begin{bmatrix}-\alpha_{\mathrm{I}} & \alpha_{\mathrm{I}}\\ \alpha_{\mathrm{II}} & -\alpha_{\mathrm{II}}\end{bmatrix}\right)\begin{bmatrix}\theta_{\mathrm{I}}\\ \theta_{\mathrm{II}}\end{bmatrix} + \begin{bmatrix}\frac{q_{\mathrm{I}}}{V_{\mathrm{I}}}\frac{1}{\xi_{\mathrm{I}}} & 0\\ 0 & \frac{q_{\mathrm{II}}}{V_{\mathrm{II}}}\frac{1}{\xi_{\mathrm{II}}}\end{bmatrix}\begin{bmatrix}\vartheta_{\mathrm{I}}^{\mathrm{in}}\\ \vartheta_{\mathrm{II}}^{\mathrm{in}}\end{bmatrix} \tag{39a}$$

$$\begin{bmatrix}\vartheta_{\mathrm{I}}^{\mathrm{out}}\\ \vartheta_{\mathrm{II}}^{\mathrm{out}}\end{bmatrix} = \begin{bmatrix}\frac{1}{\xi_{\mathrm{I}}} & 0\\ 0 & \frac{1}{\xi_{\mathrm{II}}}\end{bmatrix}\begin{bmatrix}\theta_{\mathrm{I}}\\ \theta_{\mathrm{II}}\end{bmatrix} + \begin{bmatrix}\frac{\xi_{\mathrm{I}}-1}{\xi_{\mathrm{I}}} & 0\\ 0 & \frac{\xi_{\mathrm{II}}-1}{\xi_{\mathrm{II}}}\end{bmatrix}\begin{bmatrix}\vartheta_{\mathrm{I}}^{\mathrm{in}}\\ \vartheta_{\mathrm{II}}^{\mathrm{in}}\end{bmatrix} . \tag{39b}$$

It will be shown in the following that, if the number of discretization elements is $M = 1$, it is possible to approximate the stored thermal energy E_Σ just by input/output measurements. This brings along the enormous advantage that the estimation of E_Σ is independent of the overall heat transfer coefficient U.

According to (32) and (39b) the total thermal energy of the heat exchanger model (39) reads as

$$\begin{aligned} E_\Sigma = {} & c_{p,\mathrm{I}}\varrho_{\mathrm{I}}V_{\mathrm{I}}\left(\vartheta_{\mathrm{I}}^{\mathrm{in}} + \xi_{\mathrm{I}}\left(\vartheta_{\mathrm{I}}^{\mathrm{out}} - \vartheta_{\mathrm{I}}^{\mathrm{in}}\right)\right)\\ & + c_{p,\mathrm{II}}\varrho_{\mathrm{II}}V_{\mathrm{II}}\left(\vartheta_{\mathrm{II}}^{\mathrm{in}} + \xi_{\mathrm{II}}\left(\vartheta_{\mathrm{II}}^{\mathrm{out}} - \vartheta_{\mathrm{II}}^{\mathrm{in}}\right)\right) . \end{aligned} \tag{40}$$

Under the assumption that the inlet temperatures as well as the outlet temperatures $\vartheta_{\mathrm{I}}^{\mathrm{in}}$, $\vartheta_{\mathrm{II}}^{\mathrm{in}}$, $\vartheta_{\mathrm{I}}^{\mathrm{out}}$ and $\vartheta_{\mathrm{II}}^{\mathrm{out}}$ can be measured, only ξ_{I} and ξ_{II} have to be determined. As shown in (A.5)-(A.8), ξ_{I} and ξ_{II} directly depend on the fluid velocities and on the overall heat transfer coefficient U in a nonlinear manner. However, in the stationary case U can be calculated just by the knowledge of the inlet and outlet temperatures. For this purpose, inserting (39b) into the steady state solution of (39a) yields

$$\begin{aligned} c_{p,\mathrm{I}}\varrho_{\mathrm{I}}q_{\mathrm{I}}\left(\vartheta_{\mathrm{I}}^{\mathrm{in}} - \vartheta_{\mathrm{I}}^{\mathrm{out}}\right) &= c_{p,\mathrm{II}}\varrho_{\mathrm{II}}q_{\mathrm{II}}\left(\vartheta_{\mathrm{II}}^{\mathrm{out}} - \vartheta_{\mathrm{II}}^{\mathrm{in}}\right)\\ &= Ubl\left(\theta_{\mathrm{I}} - \theta_{\mathrm{II}}\right) . \end{aligned} \tag{41}$$

In addition, with the steady state solution of the distributed-parameter model of the heat exchanger (14) the following relation can be found [7]

$$\begin{aligned} c_{p,\mathrm{I}}\varrho_{\mathrm{I}}q_{\mathrm{I}}\left(\vartheta_{\mathrm{I}}^{\mathrm{in}} - \vartheta_{\mathrm{I}}^{\mathrm{out}}\right) &= c_{p,\mathrm{II}}\varrho_{\mathrm{II}}q_{\mathrm{II}}\left(\vartheta_{\mathrm{II}}^{\mathrm{out}} - \vartheta_{\mathrm{II}}^{\mathrm{in}}\right)\\ &= Ubl\Delta\vartheta_{m,log} \end{aligned} \tag{42}$$

with the so called logarithmic mean temperature difference $\Delta\vartheta_{m,log}$. Thus, by comparing (41) and (42) the difference of θ_{I} and θ_{II} can also be obtained by the quasi-static approximation

$$\theta_{\mathrm{I}} - \theta_{\mathrm{II}} \approx \Delta\vartheta_{m,log} . \tag{43}$$

Assuming a countercurrent flow arrangement the logarithmic mean temperature difference $\Delta\vartheta_{m,log}$ results in [7]

$$\Delta\vartheta_{m,log} = \frac{\left(\vartheta_{\mathrm{I}}^{\mathrm{out}} - \vartheta_{\mathrm{II}}^{\mathrm{in}}\right) - \left(\vartheta_{\mathrm{I}}^{\mathrm{in}} - \vartheta_{\mathrm{II}}^{\mathrm{out}}\right)}{\ln\left(\frac{\vartheta_{\mathrm{I}}^{\mathrm{out}} - \vartheta_{\mathrm{II}}^{\mathrm{in}}}{\vartheta_{\mathrm{I}}^{\mathrm{in}} - \vartheta_{\mathrm{II}}^{\mathrm{out}}}\right)} , \tag{44}$$

and with (40) and (A.5) the quasi-static approximations of ξ_{I} and ξ_{II} are given by

$$\xi_{\mathrm{I}} = 1 - \xi_{\mathrm{II}} \approx \frac{\Delta\vartheta_{m,log} - \vartheta_{\mathrm{I}}^{\mathrm{in}} + \vartheta_{\mathrm{II}}^{\mathrm{out}}}{\left(\vartheta_{\mathrm{I}}^{\mathrm{out}} - \vartheta_{\mathrm{I}}^{\mathrm{in}}\right) + \left(\vartheta_{\mathrm{II}}^{\mathrm{out}} - \vartheta_{\mathrm{II}}^{\mathrm{in}}\right)} \tag{45}$$

A special case occurs if

$$\left(\vartheta_{\mathrm{I}}^{\mathrm{out}} - \vartheta_{\mathrm{II}}^{\mathrm{in}}\right) = \left(\vartheta_{\mathrm{I}}^{\mathrm{in}} - \vartheta_{\mathrm{II}}^{\mathrm{out}}\right) \tag{46}$$

since both the numerator and denominator of (44) vanish. However, if (46) is fulfilled then ξ_{I} and ξ_{II} converge to the analytical limit value of $\frac{1}{2}$.

Thus, inserting (45) into (40), it is possible to approximate the total thermal energy E_Σ just by the measurements of the inlet and outlet temperatures $\vartheta_{\mathrm{I}}^{\mathrm{in}}$, $\vartheta_{\mathrm{II}}^{\mathrm{in}}$, $\vartheta_{\mathrm{I}}^{\mathrm{out}}$ and $\vartheta_{\mathrm{II}}^{\mathrm{out}}$.

Remark: Analogously, the logarithmic mean temperature difference for the cocurrent flow arrangement is given by [7]

$$\Delta\vartheta_{m,log} = \frac{\left(\vartheta_{\mathrm{I}}^{\mathrm{out}} - \vartheta_{\mathrm{II}}^{\mathrm{out}}\right) - \left(\vartheta_{\mathrm{I}}^{\mathrm{in}} - \vartheta_{\mathrm{II}}^{\mathrm{in}}\right)}{\ln\left(\frac{\vartheta_{\mathrm{I}}^{\mathrm{out}} - \vartheta_{\mathrm{II}}^{\mathrm{out}}}{\vartheta_{\mathrm{I}}^{\mathrm{in}} - \vartheta_{\mathrm{II}}^{\mathrm{in}}}\right)} \tag{47}$$

the quasi-static approximation of ξ_{I} and ξ_{II} results in

$$\xi_{\mathrm{I}} = \xi_{\mathrm{II}} \approx \frac{\Delta\vartheta_{m,log} - \vartheta_{\mathrm{I}}^{\mathrm{in}} + \vartheta_{\mathrm{II}}^{\mathrm{in}}}{\left(\vartheta_{\mathrm{I}}^{\mathrm{out}} - \vartheta_{\mathrm{I}}^{\mathrm{in}}\right) - \left(\vartheta_{\mathrm{II}}^{\mathrm{out}} - \vartheta_{\mathrm{II}}^{\mathrm{in}}\right)} . \tag{48}$$

and converges for

$$\left(\vartheta_{\mathrm{I}}^{\mathrm{out}} - \vartheta_{\mathrm{II}}^{\mathrm{out}}\right) = \left(\vartheta_{\mathrm{I}}^{\mathrm{in}} - \vartheta_{\mathrm{II}}^{\mathrm{in}}\right) \tag{49}$$

to the analytical limit value of $\frac{1}{2}$.

Clearly, the quasi-static approximation of E_Σ is not expected to exhibit the same quality for every kind of heat exchanger. In particular, scenarios with very high residence times of the fluids inside the heat exchanger with at the same time high dynamic changes of the inputs (inlet temperatures and flow rates) could lead to an inaccurate approximation. A rigorous calculation of the exact range for which the approximation is sufficiently accurate is not trivial and out of the scope of this paper. However, many simulation and measurement studies were performed for different types of compact heat exchangers, which showed a high approximation quality. In addition, the low number of parameters required for the approximation together with the simple control law leads to a robust control behavior and to a cheap implementation.

Post-print version of the article: A. Michel and A. Kugi, “Model based control of compact heat exchangers independent of the heat transfer behavior”, *Journal of Process Control*, vol. 50, no. 11-12, pp. 1859–1868, 2014. DOI: 10.1016/j.jprocont.2014.02.003

3.5. Energy Control as Outlet Temperature Control

From an operational point of view, it is more interesting to control the outlet temperature $\vartheta_{\mathrm{I}}^{\mathrm{out}}$ than the stored thermal energy E_Σ. So it necessary to calculate the desired value of E_Σ^d in a way that the desired outlet temperature is prescribed. As already discussed, this is in general not a trivial task. However, for compact heat exchangers, the desired stored thermal Energy E_Σ^d can be determined by means of (40), (48) and (45) by replacing $\vartheta_{\mathrm{I}}^{\mathrm{out}}$ by its desired value $\vartheta_{\mathrm{I}}^{\mathrm{out},d}$. Thus E_Σ^d can be obtained from

$$\begin{aligned} E_\Sigma^d = {} & c_{p,\mathrm{I}}\varrho_{\mathrm{I}}V_{\mathrm{I}}\left(\vartheta_{\mathrm{I}}^{\mathrm{in}} + \xi_{\mathrm{I}}\left(\vartheta_{\mathrm{I}}^{\mathrm{out},d} - \vartheta_{\mathrm{I}}^{\mathrm{in}}\right)\right) \\ & + c_{p,\mathrm{II}}\varrho_{\mathrm{II}}V_{\mathrm{II}}\left(\vartheta_{\mathrm{II}}^{\mathrm{in}} + \xi_{\mathrm{II}}\left(\vartheta_{\mathrm{II}}^{\mathrm{out}} - \vartheta_{\mathrm{II}}^{\mathrm{in}}\right)\right) \ . \end{aligned} \tag{50}$$

Remark: Even if both the controller and the observer are stable, due to the nonlinearity of the heat exchanger model (14) the separation theorem does not hold and thus their interconnection is not necessarily stable. A mathematical rigorous stability proof of the closed-loop system consisting of the distributed-parameter system, the controller and the Kalman Filter or the quasi-static approximation is out of the scope of this paper. However, extensive simulation and measurement tests show a good performance and a high robustness.

Remark: The proposed energy controller does not give an integral action to the relevant outlet temperature. However, if the assumptions being made at the beginning of Section 2.1 are satisfied, in particular that there is no heat transfer with the environment, the stationary temperature error is considerably small, which was also observed in all field tests. Nevertheless, if problems with respect to stationary errors occur, there is still the possibility to include an integral part in an outer temperature control loop in cascade with the energy controller.

4. Validation

Below, the presented control strategy, the Kalman Filter and the approximation method are validated exemplary for a countercurrent compact plate heat exchanger. This results, can be directly transferred to a cocurrent flow arrangement. The validation is done by means of simulation studies and experiments on a test bench where the two fluid circuits are thermally coupled by a 1/1 pass countercurrent brazed plate heat exchanger in U-form with 40 plates. In the test bench, the temperatures are measured by means of resistance thermometers (RTDs) and the flow rates by means of turbine meters. At this point it is worth noting that in the commercialized product the flow rates are determined by means of low-cost pressure sensors. A photo of the test bench is shown in Figure 4. Note that Figure 1 exactly presents the schematic design of the experimental setup. The Nusselt correlation (5) of the used

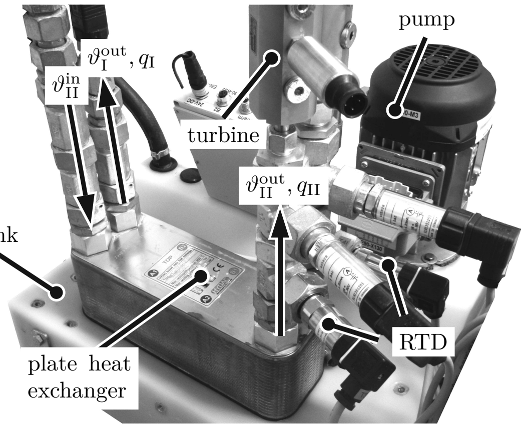

Figure 4: Test bench.

plate heat exchanger was approximated [14] in the form

$$Nu = C_{Nu} Pr^{n_{Pr}} Re^{n_{Re}} \ , \tag{51}$$

where the empirical parameters C_{Nu}, n_{Pr} and n_{Re} were identified by means of stationary measurements and are summarized with all other parameters of the heat exchanger in Table 1. Although the chosen compact plate heat exchanger has 20 parallel channels of fluid I and 19 parallel channels of fluid II, due to the repetitive conditions as regards inlet temperatures and fluid velocities, it is possible to describe the temperature of each side by only one effective temperature by introducing an effective geometric channel width b^{eff} as well as effective cross sections $A_{c,\mathrm{I}}^{\mathrm{eff}}$ and $A_{c,\mathrm{II}}^{\mathrm{eff}}$, see [14]. Thus, the plate heat exchanger can be modeled and controlled as described in the previous sections. Note that the geometric parameters in Table 1 correspond to the aforementioned effective geometric parameters. A water-glycol mixture with 44% concentration is used as fluid I and a water-glycol mixture with 40% concentration for fluid II. The fluid material parameters are listed in Table 1 for 20°C. The values for other temperatures can be found in the relevant literature, see, e.g., [17]. In order to illustrate the nonlinear relation between the overall heat transfer coefficient and the flow rates obtained from (12), (51), (6) and (17), $U(q_{\mathrm{I}}, q_{\mathrm{II}})$ is plotted for the nominal parameters and some constant q_{I} in Figure 5.

Before the performance of the proposed control concept is presented, some simulation studies concerning the estimation and approximation quality of the total thermal energy E_Σ are provided. In order to improve readability, instead of the fluid velocities u_{I} and u_{II} the corresponding flow rates q_{I} and q_{II} (cf. (17)) are used in all following studies.

Post-print version of the article: A. Michel and A. Kugi, “Model based control of compact heat exchangers independent of the heat transfer behavior”, *Journal of Process Control*, vol. 50, no. 11-12, pp. 1859–1868, 2014. DOI: 10.1016/j.jprocont.2014.02.003

Description	Symbol	Value	Unit
channel length	l	250	mm
eff. channel width	b^{eff}	3876	mm
eff. cross section side I	$A_{c,\mathrm{I}}^{\mathrm{eff}}$	3600	mm^2
eff. cross section side II	$A_{c,\mathrm{II}}^{\mathrm{eff}}$	3400	mm^2
channel hydraulic diameter	d_h	3.5	mm
plate thickness	d_p	0.5	mm
correlation parameter	C_{Nu}	0.506	
correlation parameter	n_{Pr}	0.2171	
correlation parameter	n_{Re}	0.6474	
plate thermal conductivity	k_p	15	W/m/K
plate density	ϱ_p	8000	kg/m^3
plate specific heat capacity	$c_{p,p}$	500	J/kg/K
fluid I thermal conductivity	k_I	0.45	W/m/K
fluid I density	ϱ_I	1053	kg/m^3
fluid I specific heat capacity	$c_{p,\mathrm{I}}$	3431	J/kg/K
fluid I dynamic viscosity	μ_I	3.3	mPa/s
fluid II thermal conductivity	k_II	0.45	W/m/K
fluid II density	ϱ_II	1048	kg/m^3
fluid II specific heat capacity	$c_{p,\mathrm{II}}$	3512	J/kg/K
fluid II dynamic viscosity	μ_II	2.9	mPa/s

Table 1: Heat exchanger parameters.

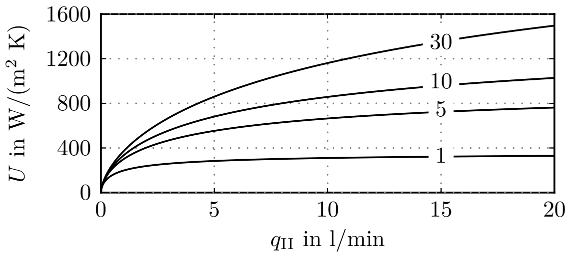

Figure 5: Nonlinear dependency of U from q_II for different values of q_I in l/min.

4.1. Simulation Results

In order to be able to evaluate the accuracy of the quasi-static approximation of the total thermal energy, a sort of worst case scenario was investigated. A big plate heat exchanger with 100 plates was simulated with low flow rates to increase the influence of the transport phenomenon and thus the residence times. At the same time, step-like changes of the inlet temperatures ($\vartheta_\mathrm{I}^{\mathrm{in}}$ and $\vartheta_\mathrm{II}^{\mathrm{in}}$) and the flow rates ($q_\mathrm{I}$ and q_II) were performed, see Figure 6(a). Two simulation models are considered, one is based on the reduced distributed-parameter model (14) neglecting the influence of the dividing plates and the other is due to (13). For both models, the finite volume method with the power balance scheme according to Appendix A is employed with $M = 50$ volume elements. Except for the effective geometric parameters $b^{\mathrm{eff}} = 9900\,\mathrm{mm}$, $A_{c,\mathrm{I}}^{\mathrm{eff}} = 9000\,\mathrm{mm}^2$ and $A_{c,\mathrm{II}}^{\mathrm{eff}} = 8820\,\mathrm{mm}^2$ all other parameters are the same as in Table 1. The time evolution of the simulated total thermal energy E_Σ (indicated by *sim.*) is compared with $\hat{E}_\Sigma$, which is obtained from the Kalman Filter (36) based on a model with $M = 10$ volume elements (indicated by *KF*), and with the quasi-static approximation (40), (44) and (45) (indicated by *QS*), see Figure 6(b) and 6(c).

It can be seen in Figure 6(b) that the estimation $\hat{E}_\Sigma$ nearly perfectly matches the simulated time evolution E_Σ of the reduced model, although the Kalman Filter only has one-fifth of the dimension of the simulation model. There is only a very small stationary error less than 0.1%. The relative error during transitions with less than 2% is also quite small. Certainly, this could have been expected because the Kalman Filter and the simulation model rely both on (14). But, if the plate dynamics are also taken into account in the simulation model, the transient estimation quality decreases, see Figure 6(c), because the heat capacity of the plates is not considered in the design of the Kalman Filter.

More interesting are the time evolutions of the quasi-static approximation of E_Σ in Figure 6(b) and 6(c). Although the residence times with up to 30 s are quite high for a compact heat exchanger, the relative error is always less than 4% even during the transitions. In addition, the approximation quality seems to be unaffected by the thermal coupling of the plates.

These results already suggest that the controller (23) with the quasi-static approximation of the total thermal energy (40), (44) and (45) may lead to a good performance of the closed-loop system in the practical application. This is justified by the fact that the simulation results considered in Figure 6 constitutes a worst-case scenario rather than a real operating condition of the plate heat exchanger, in particular with regards to the fast input changes and the high residence times of the fluid.

In the next step, the closed-loop system comprising the finite volume approximation of (13) with $M = 50$ elements, the control law (23) and the estimation of the total thermal energy E_Σ according to (36) and (40), (44) and (45), respectively, will be considered. In order to investigate the robustness of two different estimation approaches the nominal parameters of the heat transfer model of Table 1 are slightly changed as indicated in Table 2. Moreover, the dynamics of the RTD was modeled in form of a PT1 element with a rise time of 1 s. The control parameters are chosen as $\lambda_1 = 0.1$ and $\lambda_2 = 3$ for the controller with the Kalman Filter and $\lambda_1 = 0.05$ and $\lambda_2 = 2$ for the controller with the quasi-static approximation of the

Description	Symbol	Value	Unit
correlation parameter	C_{Nu}	$1.2 \cdot C_{Nu}$	
correlation parameter	n_{Pr}	$0.8 \cdot n_{Pr}$	
correlation parameter	n_{Re}	$0.8 \cdot n_{Re}$	
plate thermal conductivity	k_p	$0.9 \cdot k_p$	W/m/K
plate density	ϱ_p	$1.2 \cdot \varrho_p$	kg/m^3

Table 2: Disturbed parameters.

Post-print version of the article: A. Michel and A. Kugi, “Model based control of compact heat exchangers independent of the heat transfer behavior”, *Journal of Process Control*, vol. 50, no. 11-12, pp. 1859–1868, 2014. DOI: 10.1016/j.jprocont.2014.02.003

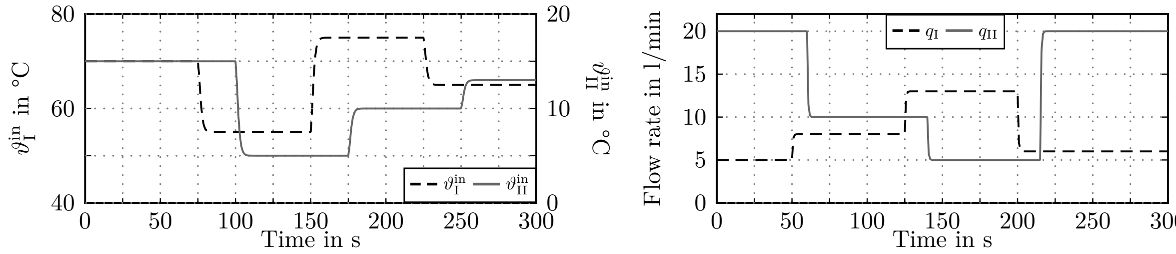

(a) Inputs.

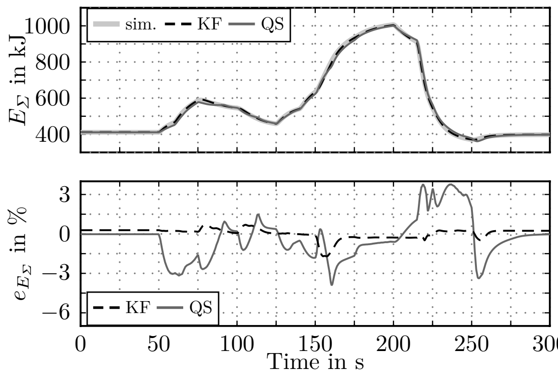

(b) Neglecting the heat capacity of the plates.

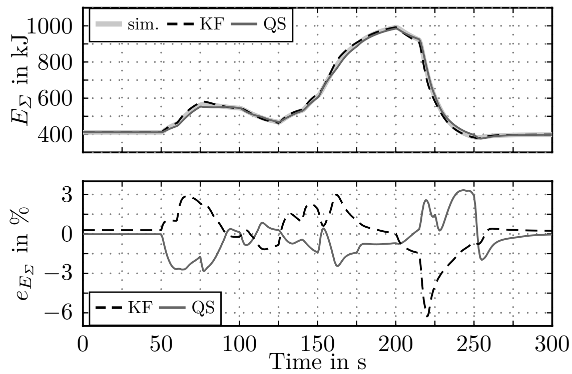

(c) Considering the heat capacity of the plates.

Figure 6: Comparison of the estimation methods for the stored thermal energy E_{Σ}.

total thermal energy. Figure 7 depicts the time evolutions of the outlet temperature $\vartheta_{\mathrm{I}}^{\mathrm{out}}$ (controlled variable), the estimation error of the total thermal energy $e_{E_{\Sigma}}$ and the corresponding flow rate q_{II} (control input) in response to a setpoint change of the desired outlet temperature. Thereby two scenarios are considered. Figure 7(a) shows the results obtained with nominal plant parameters and Figure 7(b) with disturbed plant parameters according to Table 2. Furthermore, Figure 8 depicts the time evolutions of the same quantities in response to step-like disturbances of the inlet temperatures $\vartheta_{\mathrm{I}}^{\mathrm{in}}$ and $\vartheta_{\mathrm{II}}^{\mathrm{in}}$ and the flow rate q_{I}. The results are compared to a standard PI-controller with a built-in anti-windup measure. The PI-controller was manually tuned for the nominal plant at the operating point corresponding to the first 25 s in Figure 7(a). For all simulations the superscript *KF* refers to the Kalman Filter, *QS* indicates the quasi-static approximation and *PI* refers to the PI-controller.

For nominal plant parameters, the performance of the closed-loop system with the Kalman Filter is satisfactory. But, if the parameters deviate from their nominal values the estimated total stored thermal energy $\hat{E}_{\Sigma}$ differs from its real value E_{Σ} which leads to errors of the outlet temperature. Due to the nonlinear system dynamics the closed-loop behavior of the PI-controller, which is tuned for a specific operating point, gets worse for setpoint changes already in the nominal case, see Figure 7(a) after 75 seconds. Moreover, if the plant parameters are not exactly known and disturbances are acting on the system, the PI-controller may even destabilize the system, as can be inferred from Figure 8(b) after 125 seconds. Clearly, the PI-controller could be tuned in such a way that the closed-loop system is stable for the worst-case scenario. However, this yields a humble performance for the nominal operation point of the heat exchanger. In contrast, the proposed energy controller with quasi-static approximation of E_{Σ} by means of measurements shows a good closed-loop performance in the whole operating range and is not affected by model uncertainties and disturbances at all, see the time evolutions QS in Figure 7 and 8. Having in mind that for model based control strategies a suitable Nusselt correlation has to be found and its parameters have to be determined by measurements, the practicality of the proposed approach is even more emphasized. In addition, the closed-loop behavior is unaffected against fouling, which also influences the heat transfer behavior during the lifetime of a heat exchanger.

4.2. Measurement Results

Besides the simulative validation, the proposed control methods were also implemented at the test bench described above whereby two scenarios similar to Figure 8

Post-print version of the article: A. Michel and A. Kugi, "Model based control of compact heat exchangers independent of the heat transfer behavior", *Journal of Process Control*, vol. 50, no. 11-12, pp. 1859–1868, 2014. DOI: 10.1016/j.jprocont.2014.02.003

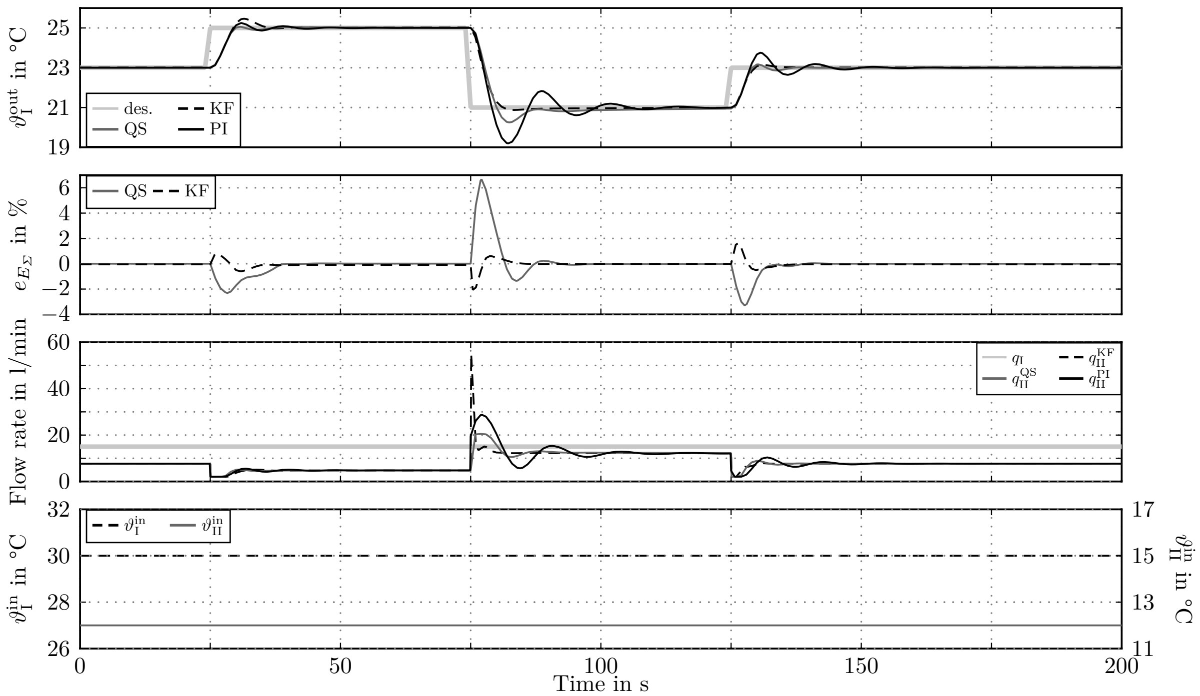

(a) Time evolutions for nominal plant parameters.

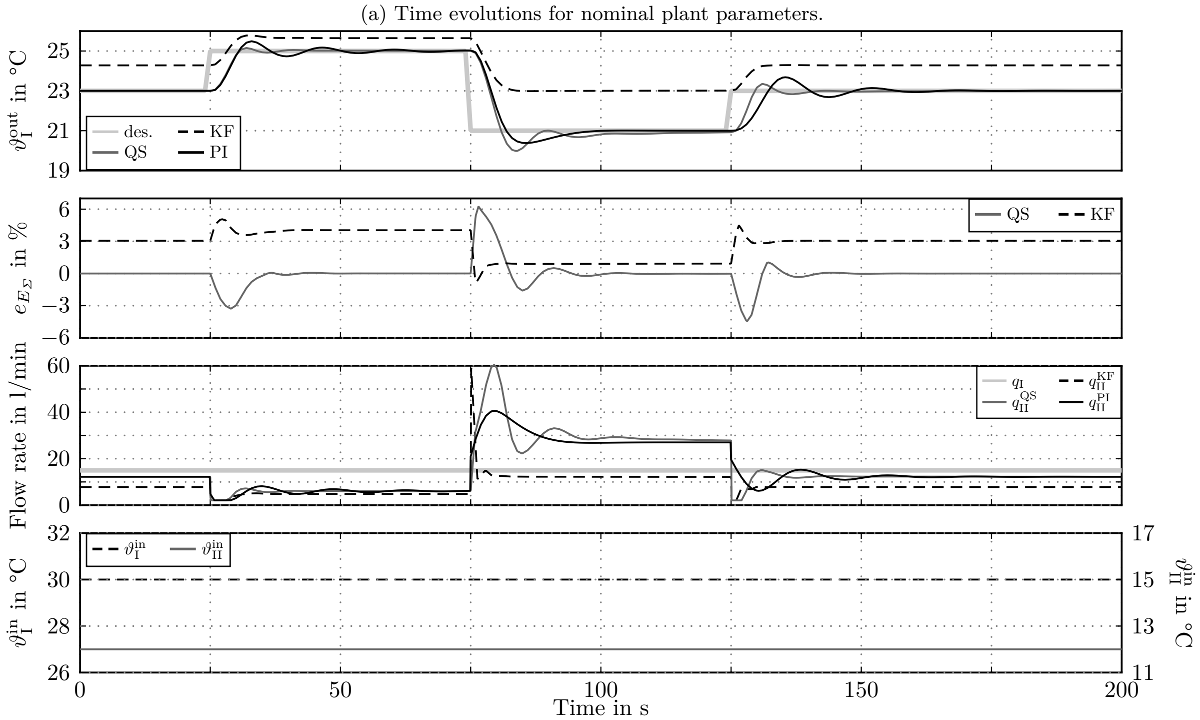

(b) Time evolutions for disturbed plant parameters.

Figure 7: Simulation results: Setpoint change.

Post-print version of the article: A. Michel and A. Kugi, "Model based control of compact heat exchangers independent of the heat transfer behavior", *Journal of Process Control*, vol. 50, no. 11-12, pp. 1859–1868, 2014. DOI: 10.1016/j.jprocont.2014.02.003
The content of this post-print version is identical to the published paper but without the publisher's final layout or copy editing.

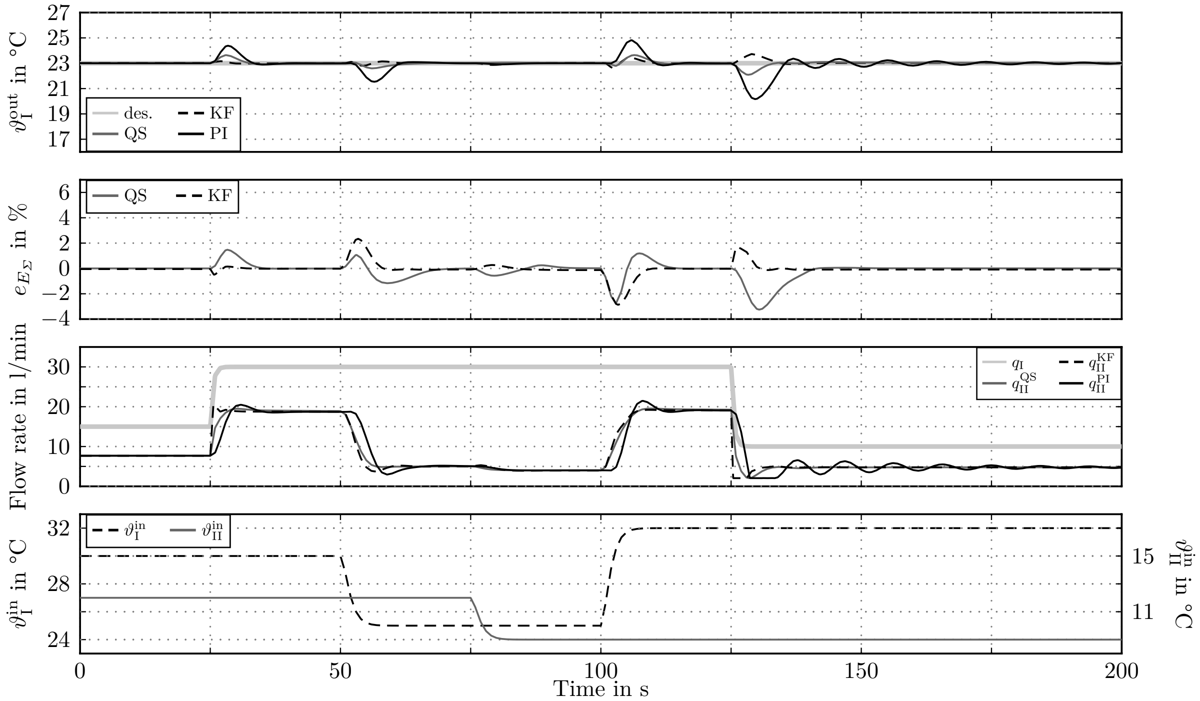

(a) Time evolutions for nominal plant parameters.

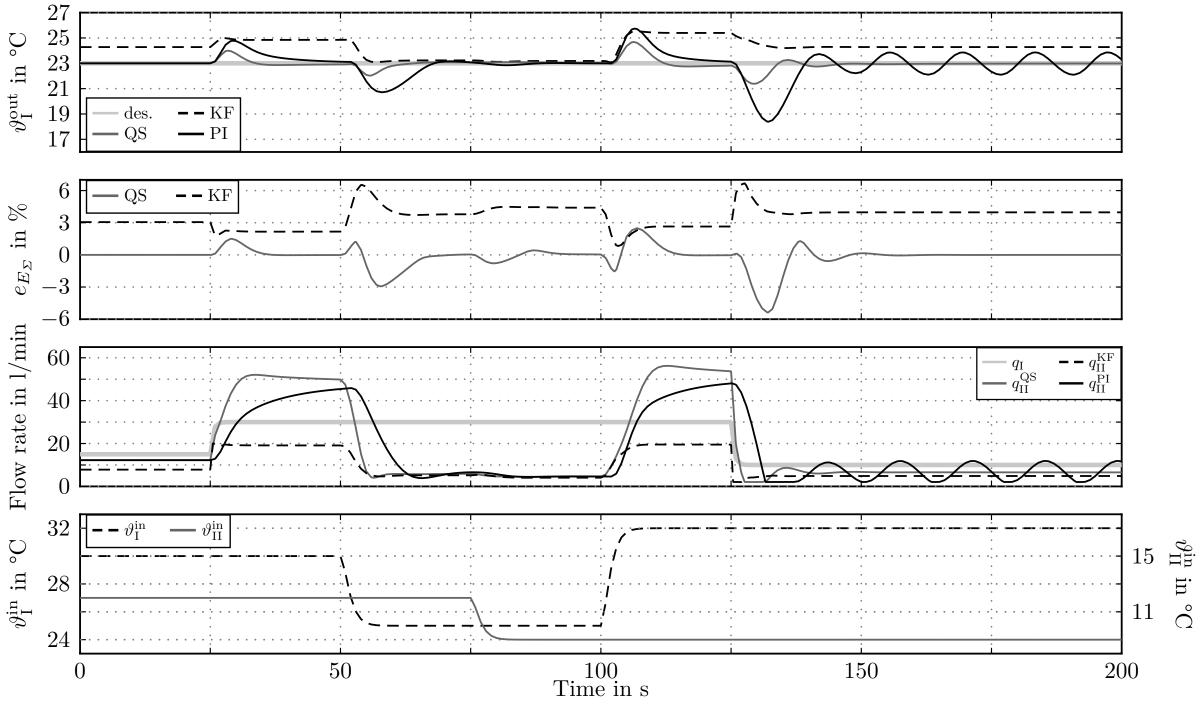

(b) Time evolutions for disturbed plant parameters.

Figure 8: Simulation results: Disturbance rejection.

Post-print version of the article: A. Michel and A. Kugi, "Model based control of compact heat exchangers independent of the heat transfer behavior", *Journal of Process Control*, vol. 50, no. 11-12, pp. 1859–1868, 2014. DOI: 10.1016/j.jprocont.2014.02.003
The content of this post-print version is identical to the published paper but without the publisher's final layout or copy editing.

and 7 were performed for nominal values of the overall heat transfer coefficient. The time evolutions of the results obtained with the Kalman Filter are depicted in Figure 9(a) and 10(a) and the time evolutions of the results obtained with the quasi-static approximation of E_Σ in Figure 9(b) and 10(b), respectively. In both cases, the simulation results are confirmed by the measurements. In the first scenario, depicted in Figure 9, the outlet temperature should be kept constant at 23 °C. Although the cooling system is exposed to large disturbances, the control error is in both cases always less than 0.5 °C. The results achieved with the Kalman Filter are slightly better. Besides, it can be seen in Figure 10 that both strategies also exhibit a good tracking behavior. The limited dynamics of the closed-loop system results from the constraints of $1 - 20$ l/min for the control input q_{II}, which was not considered in the design of the desired trajectory. It is worth noting that for the integral part in the control law (23) a simple anti-windup strategy was implemented.

Although the control strategy using the Kalman Filter shows slightly better results during disturbance rejection, it should be emphasized that its implementation was only possible, because a former identification was performed in order to determine the empirical parameters of the Nusselt correlation. Moreover, as it can be seen in Figure 10(a), the chosen Nusselt correlation is not perfect at all and there are still some stationary errors. Clearly, by adding a small integral part for the outlet temperature, this stationary error could be eliminated. But a real application will also suffer from fouling which leads to further errors in the Nusselt correlation and will make further calibrations necessary. Contrary, the control law in conjunction with the quasi-static approximation of E_Σ slightly lags behind the results obtained with the Kalman Filter, but does not need any identification or calibration, which emphasizes its benefits in practical applications.

5. Conclusions

In this paper, a model based control strategy for a compact fluid-fluid heat exchanger was developed where the total thermal energy stored in the fluids of the heat exchanger was used as control variable instead of the outlet temperature.

Since the total thermal energy cannot be directly measured two approaches for its estimation were presented. At first a Kalman Filter was designed based on a finite volume discretization of the underlying distributed-parameter system utilizing the so called power balance scheme. In order to render the control concept independent of the heat transfer model, which usually relies on semi-empirical considerations and requires extensive identifications, a second quasi-static approach for the estimation of the total energy was employed. Simulation and measurement results for an industrial 1/1 pass countercurrent brazed plate heat exchanger demonstrate the feasibility of the proposed approach.

It should be emphasized that this control concept can be applied to any kind of compact heat exchanger and does not need any former identification. Moreover, the performance does not deteriorate over the lifetime of the heat exchanger for instance due to fouling effects and is independent of changes in the coolant supply system. The only price one has to pay for this robust behavior is that the inlet and outlet temperatures and the flow rates on both sides of the heat exchanger have to be measured.

Acknowledgement

The authors kindly thank the HYDAC Cooling GmbH for the financial and technical support.

Appendix A. Finite Volume Discretization using the Power Balance Scheme

First, the spatial domain is divided into M volume elements of length $\Delta l = \frac{l}{M}$ and then integrated over the length l. Thereby the temperature inside each volume element is assumed to be constant. Applying this to (14) and demanding that the resulting residuum of every volume element vanishes, leads to the lumped-parameter system

$$\frac{\mathrm{d}\theta_{i,\mathrm{I}}}{\mathrm{d}t} + \frac{u_{\mathrm{I}}}{\Delta l}\,\vartheta_{\mathrm{I}}\big|_{(i-1)\Delta l}^{i\Delta l} + \alpha_{\mathrm{I}} U\left(\theta_{i,\mathrm{I}} - \theta_{i,\mathrm{II}}\right) = 0\ , \qquad \text{(A.1a)}$$

$$\frac{\mathrm{d}\theta_{i,\mathrm{II}}}{\mathrm{d}t} + \frac{u_{\mathrm{II}}}{\Delta l}\,\vartheta_{\mathrm{II}}\big|_{(i-1)\Delta l}^{i\Delta l} + \alpha_{\mathrm{II}} U\left(\theta_{i,\mathrm{II}} - \theta_{i,\mathrm{I}}\right) = 0 \qquad \text{(A.1b)}$$

with $i = 1, \ldots, M$ and the temperature mean values

$$\theta_{i,k} = \frac{1}{\Delta l}\int_{(i-1)\Delta l}^{i\Delta l} \vartheta_{i,k}\mathrm{d}x, \qquad k \in \{\mathrm{I}, \mathrm{II}\}\ . \qquad \text{(A.2)}$$

In order to calculate the temperatures at the element borders, $\vartheta_{\mathrm{I}}(i\Delta l)$ and $\vartheta_{\mathrm{II}}(i\Delta l)$, $i = 0, \ldots, M$, several numerical approaches can be found in literature, see, e.g., [5]. In this paper, the power balance scheme is used which is explained in detail in [14]. Thereby, the temperatures at the element borders are approximated in such a way that the stationary solution of the finite volume model is identical to the stationary solution of (14). This can be achieved by the following interpolation, see [14]

$$\vartheta_k(i\Delta l) = \begin{cases} \frac{1}{\xi_k}\theta_{i,k} + \frac{\xi_k - 1}{\xi_k}\vartheta_k((i-1)\Delta l) & \text{for} \quad u_k > 0 \\ \frac{1}{\xi_k}\theta_{i,k} + \frac{\xi_k - 1}{\xi_k}\vartheta_k((i+1)\Delta l) & \text{for} \quad u_k < 0 \end{cases} \qquad \text{(A.3)}$$

with

$$i = \begin{cases} 1, \ldots, M & u_k > 0 \\ 0, \ldots, M-1 & u_k < 0\ , \end{cases} \qquad \text{(A.4)}$$

$k \in \{\mathrm{I}, \mathrm{II}\}$ and the boundary conditions (3). The coefficients ξ_{I} and ξ_{II} are related depending on the sign of

Post-print version of the article: A. Michel and A. Kugi, "Model based control of compact heat exchangers independent of the heat transfer behavior", *Journal of Process Control*, vol. 50, no. 11-12, pp. 1859–1868, 2014. DOI: 10.1016/j.jprocont.2014.02.003

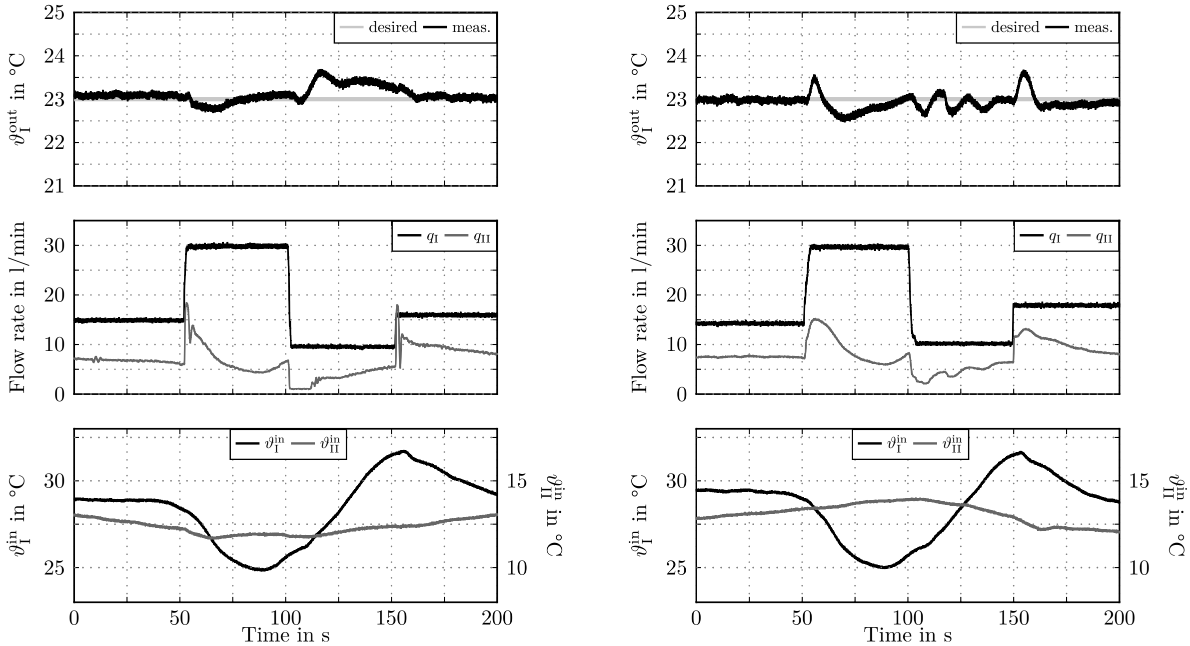

(a) Measurement results obtained with the Kalman Filter.

(b) Measurement results obtained with the quasi-static approximation.

Figure 9: Measurement results: Disturbance rejection.

the fluid velocities. For countercurrent flow ($\operatorname{sign}(u_{\mathrm{II}}) = -\operatorname{sign}(u_{\mathrm{I}})$) ξ_{II} is given in the form

$$\xi_{\mathrm{II}} = 1 - \xi_{\mathrm{I}} \tag{A.5}$$

and for cocurrent flow ($\operatorname{sign}(u_{\mathrm{II}}) = \operatorname{sign}(u_{\mathrm{I}})$)

$$\xi_{\mathrm{II}} = \xi_{\mathrm{I}} \;, \tag{A.6}$$

with ξ_{I} for $u_{\mathrm{I}} > 0$ according to

$$\xi_{\mathrm{I}} = \frac{\exp \varGamma\,(\varGamma - 1) + 1}{\varGamma\,(\exp \varGamma - 1)} \tag{A.7}$$

and

$$\varGamma = \frac{\alpha_{\mathrm{I}} U \varDelta l}{u_{\mathrm{I}}} + \frac{\alpha_{\mathrm{II}} U \varDelta l}{u_{\mathrm{II}}} \;. \tag{A.8}$$

Utilizing the power balance scheme, the lumped-parameter model (A.1) can be summarized in the form

$$\begin{aligned} \frac{\mathrm{d}}{\mathrm{d}t}\boldsymbol{\theta} &= \mathbf{A}(\mathbf{u})\boldsymbol{\theta} + \mathbf{B}(\mathbf{u})\boldsymbol{\vartheta}^{\mathrm{in}} \\ \boldsymbol{\vartheta}^{\mathrm{out}} &= \mathbf{C}(\mathbf{u})\boldsymbol{\theta} + \mathbf{D}(\mathbf{u})\boldsymbol{\vartheta}^{\mathrm{in}} \;, \end{aligned} \tag{A.9}$$

with the state vector $\boldsymbol{\theta} = [\boldsymbol{\theta}_{\mathrm{I}}, \boldsymbol{\theta}_{\mathrm{II}}]^{\mathrm{T}}$, the input vectors $\mathbf{u} = [u_{\mathrm{I}}, u_{\mathrm{II}}]^{\mathrm{T}}$ and $\boldsymbol{\vartheta}^{\mathrm{in}} = \left[\vartheta_{\mathrm{I}}^{\mathrm{in}}, \vartheta_{\mathrm{II}}^{\mathrm{in}}\right]^{\mathrm{T}}$ and the output vector $\boldsymbol{\vartheta}^{\mathrm{out}} = [\vartheta_{\mathrm{I}}^{\mathrm{out}}, \vartheta_{\mathrm{II}}^{\mathrm{out}}]^{\mathrm{T}}$. The system matrices can be determined in the form

$$\mathbf{A}(\mathbf{u}) = \mathbf{A}_c(\mathbf{u}) + U(\mathbf{u})\mathbf{A}_t \tag{A.10a}$$

$$\mathbf{B}(\mathbf{u}) = \begin{bmatrix} \frac{|u_{\mathrm{I}}|}{\varDelta l}\mathbf{b}_{\mathrm{I}}(u_{\mathrm{I}}) & \mathbf{0}^{M\times 1} \\ \mathbf{0}^{M\times 1} & \frac{|u_{\mathrm{II}}|}{\varDelta l}\mathbf{b}_{\mathrm{II}}(u_{\mathrm{II}}) \end{bmatrix} \tag{A.10b}$$

$$\mathbf{C}(\mathbf{u}) = \begin{bmatrix} \mathbf{c}_{\mathrm{I}}^{\mathrm{T}}(u_{\mathrm{I}}) & \mathbf{0}^{1\times M} \\ \mathbf{0}^{1\times M} & \mathbf{c}_{\mathrm{II}}^{\mathrm{T}}(u_{\mathrm{II}}) \end{bmatrix} \tag{A.10c}$$

$$\mathbf{D}(\mathbf{u}) = \begin{bmatrix} d_{\mathrm{I}}(u_{\mathrm{I}}) & 0 \\ 0 & d_{\mathrm{II}}(u_{\mathrm{II}}) \end{bmatrix} \tag{A.10d}$$

with

$$\mathbf{A}_c(\mathbf{u}) = \begin{bmatrix} -\frac{|u_{\mathrm{I}}|}{\varDelta l}\mathbf{A}_{c,\mathrm{I}}(u_{\mathrm{I}}) & \mathbf{0}^{M\times M} \\ \mathbf{0}^{M\times M} & -\frac{|u_{\mathrm{II}}|}{\varDelta l}\mathbf{A}_{c,\mathrm{II}}(u_{\mathrm{II}}) \end{bmatrix} \tag{A.11}$$

$$\mathbf{A}_t = \begin{bmatrix} -\alpha_{\mathrm{I}}\mathbf{I}^M & \alpha_{\mathrm{I}}\mathbf{I}^M \\ \alpha_{\mathrm{II}}\mathbf{I}^M & -\alpha_{\mathrm{II}}\mathbf{I}^M \end{bmatrix} \;, \tag{A.12}$$

where the discretization matrices depend on the sign of

Post-print version of the article: A. Michel and A. Kugi, “Model based control of compact heat exchangers independent of the heat transfer behavior”, *Journal of Process Control*, vol. 50, no. 11-12, pp. 1859–1868, 2014. DOI: 10.1016/j.jprocont.2014.02.003
The content of this post-print version is identical to the published paper but without the publisher’s final layout or copy editing.

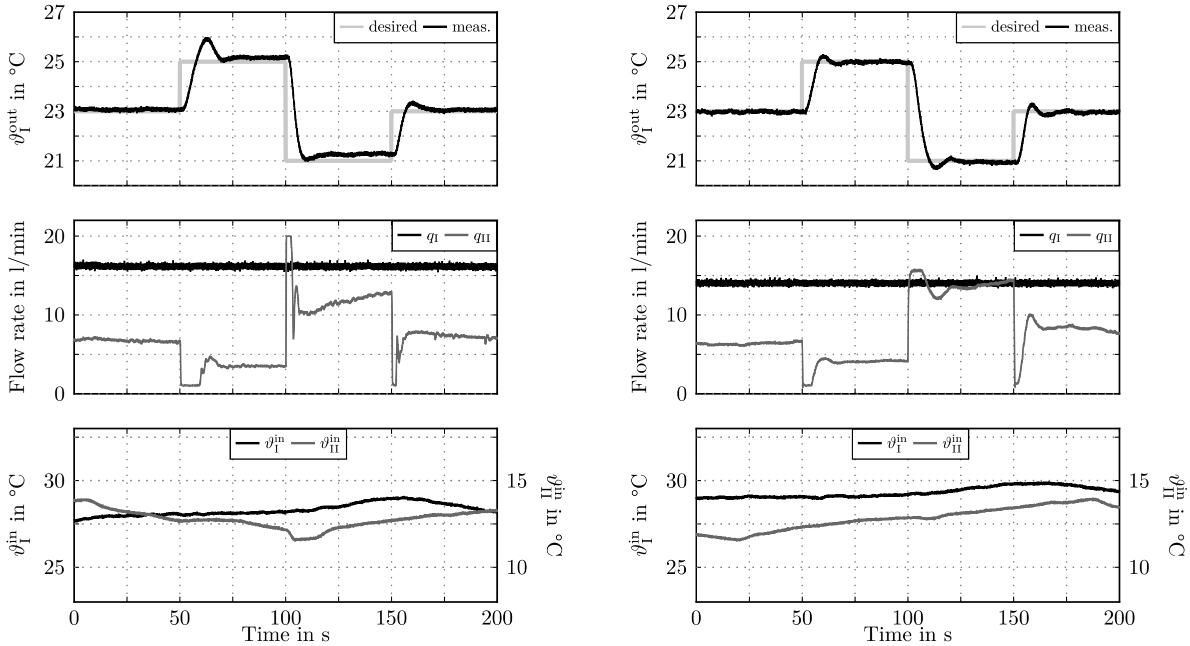

(a) Measurement results obtained with the Kalman Filter.

(b) Measurement results obtained with the quasi-static approximation.

Figure 10: Measurement results: Setpoint change.

the particular fluid velocity and calculate according to

$$\mathbf{A}_{c,k}(u_k) = \begin{cases} \mathbf{A}^1_{k,+} - \mathbf{A}^2_{k,+} & \text{for} \quad u_k > 0 \\ \mathbf{A}^1_{k,-} - \mathbf{A}^2_{k,-} & \text{for} \quad u_k < 0 \end{cases} \tag{A.13a}$$

$$\mathbf{b}_k(u_k) = \begin{cases} \mathbf{b}_{k,+} & \text{for} \quad u_k > 0 \\ \mathbf{b}_{k,-} & \text{for} \quad u_k < 0 \end{cases} \tag{A.13b}$$

$$\mathbf{c}_k(u_k) = \begin{cases} \mathbf{c}_{k,+} & \text{for} \quad u_k > 0 \\ \mathbf{c}_{k,-} & \text{for} \quad u_k < 0 \end{cases} \tag{A.13c}$$

$$d_k = \left(\frac{\xi_k - 1}{\xi_k} \right)^M \tag{A.13d}$$

with the entries of the matrices

$$\begin{aligned} \mathbf{A}^l_{k,-}(i-(l-1), j) &= \begin{cases} \frac{1}{\xi_k}\left(\frac{\xi_k - 1}{\xi_k}\right)^{(j-i)} & \text{for} \quad \begin{array}{l} i = l, \dots, M, \\ j = i, \dots, M \end{array} \\ 0 & \text{else} \end{cases} \\ \mathbf{b}_{k,-}(i) &= \frac{1}{\xi_k}\left(\frac{\xi_k - 1}{\xi_k}\right)^{(M-i)} \quad \text{for } i = 1, \dots, M \\ \mathbf{c}_{k,-}(i) &= \frac{1}{\xi_k}\left(\frac{\xi_k - 1}{\xi_k}\right)^{(i-1)} \quad \text{for } i = 1, \dots, M \end{aligned} \tag{A.14}$$

and

$$\begin{aligned} \mathbf{A}^l_{k,+}(i,j) &= \mathbf{A}^l_{k,-}(M-(i-1), M-(j-1)) \\ \mathbf{b}_{k,+}(i) &= \mathbf{b}_{k,-}(M-(i-1)) \\ \mathbf{c}_{k,+}(i) &= \mathbf{c}_{k,-}(M-(i-1)) \end{aligned} \tag{A.15}$$

for $k \in \{\mathrm{I}, \mathrm{II}\}$. Thereby, $\mathbf{M}(i,j)$ denotes the element in row i and column j of the matrix $\mathbf{M}$, $\mathbf{I}^a \in \mathbb{R}^{a \times a}$ is the identity matrix and $\mathbf{0}^{a \times b} \in \mathbb{R}^{a \times b}$ denotes the zero matrix.

References

[1] Al-Dawery, S. K., Alrahawi, A. M., & Al-Zobai, K. M. (2012). Dynamic modeling and control of plate heat exchanger. *International Journal of Heat and Mass Transfer*, *Vol. 55*, 6873–6880.

[2] Álvarez, J. D., Yebra, L. J., & Berenguel, M. (2007). Repetitive control of tubular heat exchangers. *Journal of Process Control*, *Vol. 17*, 689–701.

[3] Baehr, H. D., & Stephan, K. (2006). *Heat and Mass Transfer*. (2nd ed.). Berlin / Heidelberg: Springer.

[4] Bagui, F., Abdelghani-Idrissi, M. A., & Chafouk, H. (2004). Heat exchanger Kalman filtering with process dynamic acknowledgement. *Computers & Chemical Engineering*, *Vol. 28*, 1465–1473.

[5] Ferziger, J. H., & Perić, M. (2002). *Computational Methods for Fluid Dynamics*. (3rd ed.). Berlin / Heidelberg: Springer-Verlag.

[6] Fischer, M., Nelles, O., & Isermann, R. (1998). Adaptive predictive control of a heat exchanger based on a fuzzy model. *Control Engineering Practice*, *Vol. 6*, 259–269.

[7] Holman, J. P. (2010). *Heat Transfer*. (10th ed.). New York: McGraham-Hill.

Post-print version of the article: A. Michel and A. Kugi, "Model based control of compact heat exchangers independent of the heat transfer behavior", *Journal of Process Control*, vol. 50, no. 11-12, pp. 1859–1868, 2014. DOI: 10.1016/j.jprocont.2014.02.003

The content of this post-print version is identical to the published paper but without the publisher's final layout or copy editing.

[8] Jonsson, G. R., Lalot, S., Palsson, O. P., & Desmet, B. (2007). Use of extended Kalman filtering in detecting fouling in heat exchangers. *International Journal of Heat and Mass Transfer*, *Vol. 50*, 2643–2655.

[9] Kakaç, S., & Liu, H. (2002). *Heat Exchangers - Selection, Rating and Thermal Design*. London / New York / Washington D.C.: CRC Press.

[10] Katayama, T., Itho, T., Ogawa, M., & Yamamoto, H. (1990). Optimal Tracking Control of a Heat Exchanger with Change in Load Condition. In *Proceedings of the 29th Conference on Decison and Control* (pp. 1584–1589). Honolulu, Hawaii.

[11] Maidi, A., Diaf, M., & Corriou, J. P. (2009). Boundary Geometric Control of a Counter-current Heat Exchanger. *Journal of Process Control*, *Vol. 19*, 297–313.

[12] Maidi, A., Diaf, M., & Corriou, J. P. (2010). Boundary control of a parallel-flow heat exchanger by input–output linearization. *Journal of Process Control*, *Vol. 20*, 1161–1174.

[13] Malleswararao, Y. S. N., & Chidambaram, M. (1992). Nonlinear controllers for a heat exchanger. *Journal of Process Control*, *Vol. 2*, 17–21.

[14] Michel, A., & Kugi, A. (2013). Accurate low-order dynamic model of a compact plate heat exchanger. *International Journal of Heat and Mass Transfer*, *Vol. 61*, 323–331.

[15] Shah, R. K., & Sekulić, D. P. (2003). *Fundamentals of Heat Exchanger Design*. New Jersey: John Wiley & Sons, Inc.

[16] Vazquez, R., Krstic, M., & Coron, J. M. (2011). Backstepping Boundary Stabilization and State Estimation of a 2x2 Linear Hyperbolic System. In *Proceedings of the IEEE Conference on Decision and Control and European Control Conference (CDC-ECC)* (pp. 4937–4942). Orlando, FL, USA.

[17] VDI-Gesellschaft Verfahrenstechnik und Chemieingenieurwesen (2010). *VDI Heat Atlas*. (2nd ed.). Berlin/Heidelberg: Springer.

[18] Woittennek, F., Rudolph, J., & Knüppel, T. (2009). Flatness Based Trajecory Planning for a semi-linear Hyperbolic System of First Order P.D.E. Modeling a Tubular Reactor.

[19] Zavala-Río, A., Astorga-Zaragoza, C. M., & Hernández-González, O. (2009). Bounded positive control for double-pipe heat exchangers. *Control Engineering Practice*, *Vol. 17*, 136–145.

Post-print version of the article: A. Michel and A. Kugi, "Model based control of compact heat exchangers independent of the heat transfer behavior", *Journal of Process Control*, vol. 50, no. 11-12, pp. 1859–1868, 2014. DOI: 10.1016/j.jprocont.2014.02.003
The content of this post-print version is identical to the published paper but without the publisher's final layout or copy editing.